The construction of 2DV morphodynamic models in double inlet systems

Wytze Roël

September 2021

Abstract

The change in sea beds in double inlet systems is caused by a complex combination of factors such as sea level dynamics, water movement and suspended sediment in the water. The unchanged water depth, the equilibrium seabed, in inlet systems is important to know for shipping near harbours and wildlife in nature reserves.

An idealized exploratory version of this complex system of morphodynamics to find the equilibrium solutions is usually modelled in a depth- and width-averaged way, which removes the vertical structure. Hence I will investigate if it is possible to model the system in a width-averaged two-dimensional way with the vertical structure intact and what are the consequences of retaining the vertical structure?

To investigate this the construction of a two-dimensional model is described and the solution methods posed. Following this the resulting equilibrium sea beds are compared to the equilibrium sea beds found in depth-averaged one-dimensional models to ascertain the importance of the vertical structure.

It was found that adding the vertical structure makes the resulting governing equations of the model more complex but can be solved with perturbation techniques. Furthermore, for specific sets of parameters describing the system it is possible to have multiple equilibrium sea beds, which suggests the existence of bifurcations. Finally, it is possible to find a relation between the 1-dimensional and 2-dimensional governing equations that results in both models producing the same results.

Concluding, two-dimensional models compared to one-dimensional models add an extra layer of complexity which allows for bifurcations but makes the model computatively more expensive. Instead, using the relation found in this paper in a one-dimensional model is preferred as in theory it results in the same equilibrium sea beds found.

Contents

1 Introduction **3**
- 1.1 Introduction . . . 3
  - 1.1.1 Inlet system . . . 4
  - 1.1.2 Morphodynamical model . . . 9
  - 1.1.3 Previous research . . . 10
- 1.2 Research questions . . . 11

2 The mathematical model **13**
- 2.1 Geometry . . . 15
- 2.2 Morphodynamic Model . . . 15
  - 2.2.1 Water motion . . . 16
  - 2.2.2 Sediment concentration . . . 20
  - 2.2.3 Sea bed evolution . . . 22
- 2.3 Solution methods . . . 23
  - 2.3.1 Minimization . . . 24
  - 2.3.2 Iterative method . . . 25
  - 2.3.3 Hybrid method . . . 27
- 2.4 Depth-averaged version . . . 27
  - 2.4.1 Conversion factor . . . 27
  - 2.4.2 Depth-averaged model . . . 28

3 Results **30**
- 3.1 Morphodynamics on an idealized domain . . . 31
  - 3.1.1 Water motion . . . 31
  - 3.1.2 Sediment concentration . . . 33
  - 3.1.3 Sea bed evolution . . . 34
  - 3.1.4 Equilibrium solutions . . . 35
- 3.2 Parameter sensitivity . . . 36
  - 3.2.1 Friction with the sea bed . . . 37
  - 3.2.2 Settling velocity . . . 39
  - 3.2.3 Vertical eddy viscosity and diffusivity coefficient . . . 41
  - 3.2.4 Relative phase difference . . . 44
  - 3.2.5 Length of inlet system . . . 48
  - 3.2.6 Depth of inlet system . . . 50

3.3 Comparison with depth-averaged models 52
3.3.1 Water motion 52
3.3.2 Sediment concentration 55
3.3.3 Equilibrium solutions 56

4 Conclusion and discussion **58**
4.1 Conclusion 58
4.1.1 Two-dimensional model for morphodynamics 58
4.1.2 Comparison with one-dimensional models 59
4.2 Discussion 59

Appendices **61**

A Appendix A **62**
A.1 Width-averaged model 62
A.1.1 Width-averaged shallow water equations 62
A.1.2 Width-averaged concentration equation 67
A.1.3 Morphodynamic Equilibrium Condition 69

Chapter 1

Introduction

1.1 Introduction

Tidal inlets are connections between the open sea and back barrier basins that are otherwise sheltered from the open sea. These inlets are found in many shallow coastal regions around the world and are typically characterized by complex water motion, caused by the tides, wind and density gradient, resulting in transport of sediment and changes in bathymetry.

The evolution of the sea bed can be computed using so-called morphodynamic models in which the hydrodynamics and sediment concentration are dynamically coupled to the bed evolution. This allows the assessment of the temporal bed changes. Apart from this information concerning the transient behaviour, a relevant question is whether there exist so-called morphodynamical equilibria for these systems. A sea bed is considered in equilibrium when the bottom does not change any more, assuming outside forces are constant. Such an equilibrium can thus be seen as the shape to which the sea bed will eventually evolve.

There are many scenarios why the knowledge of the existence and characteristics of equilibria is important. First of all, a busy sea port which is connected to the open sea through a tidal inlet system relies on the tidal inlet system being of certain depth.
When the tidal inlet system is dredged to make it possible for larger ships to travel through the inland ports, it is important to know how long it takes for the sea bed to change such that the channel needs to be dredged again.

Second, for nature reserves, the fauna that breeds and lives in these areas depends on specific characteristics of the breeding grounds, such as shallow waters. However, these areas have often been changed in such a way that the sea bed is not in equilibrium any more. Hence, an important question concerns whether the resulting sea bed will allow the current fauna to thrive in these nature re-

serves.

Not only human interventions, but also other incidents can have a lasting effect on these systems. Climate change, for instance, could cause a permanent or temporary rise in sea level. In view of this, it is important to assess the effects of external forces on the equilibrium profiles. This is particularly important if more than one morphodynamical equilibrium exists for the same forcing conditions.
If this is the case it is possible that also temporary changes in outside forces like hurricanes cause the sea bed to evolve to a different equilibrium, which can have huge economical and ecological consequences.

1.1.1 Inlet system

A tidal inlet system is an opening in the shoreline connecting the open sea and a body of water that is sheltered by barrier islands on the seaward side and mainland on the other side. Tides play an important role in forcing the water motion in these inlet systems. Due to the water motion, sediment is eroded from the bed, transported and again deposited on the bed, resulting in a changing bathymetry.

The tides consist of many different components, like the semi-diurnal M_2 tidal constituent and its first overtide M_4. Also, the sea level is highly influenced by other factors like the wind and seasons. The semi-diurnal tidal constituent is the most important forcing component for the systems we consider. The temporal behaviour of the resulting water velocity and sediment concentration is directly related to the period of this semi-diurnal tide. However, significant evolution of the sea bed occurs only after many semi-diurnal tidal cycles; hence the sea bed evolution occurs on a much larger time scale.

Furthermore, there are two types of inlet systems: a single inlet system only connected to the sea by one opening; and a multiple inlet system which is connected to the sea by more than one tidal inlet. In the next section an example of a single and a double inlet system is discussed in detail. A double inlet system is a system that is connected by two inlets to the sea.

Single inlet system

An example of a single inlet system is the Frisian inlet system. The tidal inlet of this system is located between the islands of Ameland and Schiermonnikoog in the Wadden Sea, see Figure 1.1. It drains one of the back barrier basins of the Wadden Sea. In 1969 the area of the back barrier basin was reduced considerably as the Lauwers Sea was drained for reclamation of land.
Because of this sudden change, the sea bed between the barrier islands Ameland and Schiermonnikoog and the Lauwerszee was no longer in equilibrium and the

Figure 1.1: Single inlet system at the Lauwerszee

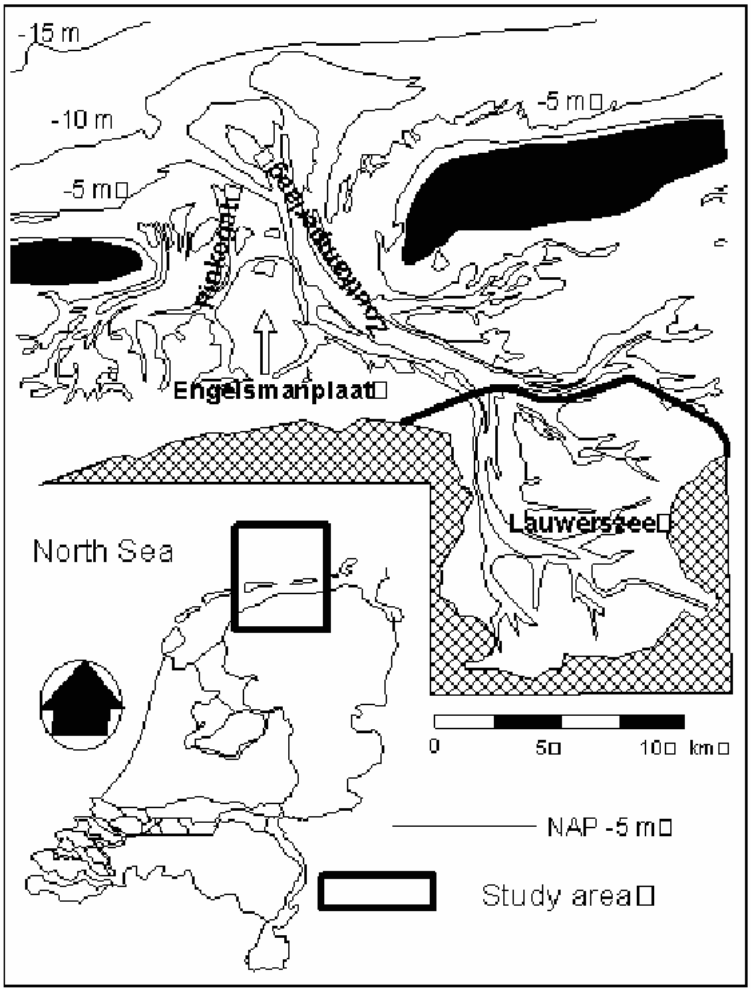

system started to evolve on the morphodynamic time-scale.
Because the tidal inlet system is only connected to the sea at one side, it is to be expected that the sediment will accumulate at the landward side and eventually will rise until the sea bed reaches the water surface.

Figure 1.2: Double inlet system in the Marsdiep-Vlie estuary

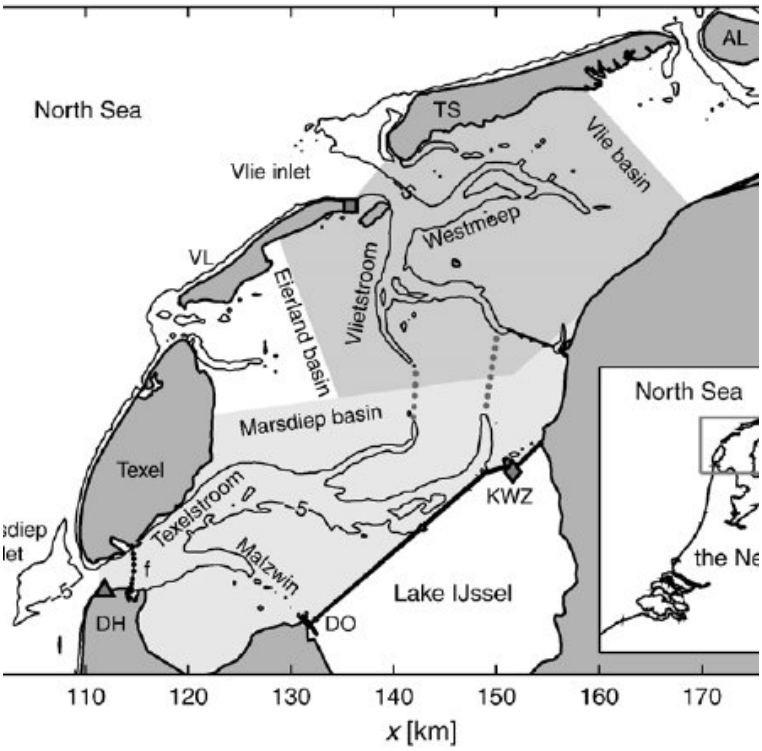

Double inlet system

A double inlet system is a system where the back barrier basin is connected to the sea by two inlets. An example of such a system is the Marsdiep-Vlie inlet system, see Figure 1.2. One inlet is found between Texel and the mainland at Den Helder and the other inlet of this system is located between Terschelling and Vlieland. Like the Frisian inlet system, this inlet system is not used by large ships and is in general not dredged for commercial use because it is part of the Wadden Sea Region, which is a nature reserve.

Because both ends of this tidal inlet system are connected to the sea, the water in the system can travel from one end to the other. The water motion depends on the difference in sea level between the inlets, as tidal waves can travel in both directions and interfere in the basin itself. As the tidal waves move along the coastline, the sea level between the inlets will usually vary slightly, resulting in a different phasing of the tidal signal and possibly a different tidal amplitude. When the two inlets are close together, the difference in sea level will usually be characterized by a small phase difference.
The phase and amplitude difference in sea level between the two inlets in the

Figure 1.3: Phase difference in sea level between the two inlets of Marsdiep-Vlie inlet system

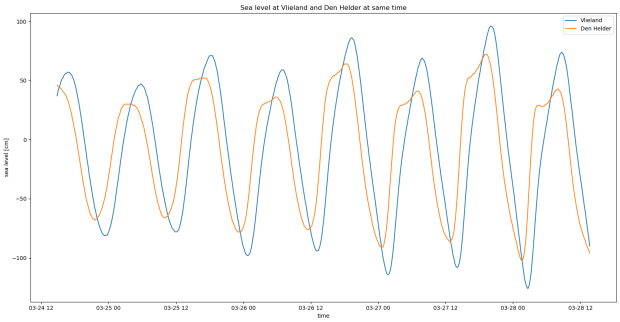

Marsdiep-Vlie inlet system is displayed in figure 1.3. The data for this plot is obtained from the Department of Waterways and Public Works. [1]

1.1.2 Morphodynamical model

To capture the temporal behaviour of this type of system various types of models can be used. Restricting our attention to model based on first physical principles, we can distinguish two types: simulation and exploratory models. Both models are based on physical laws. Simulation models include all known processes and strive to represent the morphodymanic evolution as accurately as possible [7]. These models make use of numerical integration techniques. Exploratory models are using simplified model formulations, and can be used to evaluate specific phenomena in isolation.

Ideally, simulation models are the best way to model morphodynamics as all known processes are included. However, the inclusion of all processes makes the computations very expensive because the underlying governing equations are complex resulting in long calculation times. Furthermore, the models are so complex that it is often hard to explain why the model returned a certain result. These two drawbacks make it difficult to assess whether small changes in initial conditions or physical parameters can result in drastically different morphodynamic behaviour.

The model used in this research is an exploratory model and aims to investigate the sea bed evolution of inlet systems by focusing on dominant processes. When constructing an exploratory model, only the most important phenomena are used in the calculations. This results in a model that is easier in use.

Using exploratory models in morphodynamics has the benefit that previous exploratory models, that have been deemed as correctly modelling morphodynamics, can be easily expanded to include more physical processes. The impact of this expansion can be quantified easily by comparing the results of the expanded model with results of the previous model.
A drawback of this research method is that the results may not be representative of behaviour in reality, because not all known processes are included in the morphodynamical model. For this only simulation models can provide accurate predictions.

Identifying the most important phenomena

To obtain insights in the importance of the various terms in the equations, the equations are nondimensionalized. This is a commonly used method in mathematics which scales physical quantities with characteristic scales. This results in dimensionless numbers that indicate the magnitude of the various terms. In this way it becomes clear which terms in the equations are the dominant ones. This process is sometimes called scaling.

Perturbation methods are used in mathematics to find approximate solutions in equations that can not be solved exactly. By finding the most important terms

in the equations and first solving the equations with those terms, perturbation methods can be used to approximate the solution of equations. If an additional layer is then added to also solve the equations for the less important terms, an asymptotic expansion of the actual solution of the set of equations can be constructed.

1.1.3 Previous research

In the field of exploratory models research has been conducted on both single and double inlets. Often perturbation techniques are used to acquire approximate solutions of the exploratory model. Furthermore, spatial averaging is often used to further simplify the models.
In spatial averaging, one or two dimensions, usually the width and depth are averaged in the governing equations. The flow in the along-channel direction is obviously the most important direction. The flow over the width and depth are of less importance.
The importance of the width and depth can be investigated with exploratory modelling. The disadvantage of averaging over a spatial direction is that only averaged quantities are retained, and possible correlations are taken into account in a parametric way. In this way the spatial structure of that direction is not resolved. For example, when averaging over the depth, there is no information of the water velocity and sediment concentration at the sea bed, only depth-averaged quantities are obtained.

Schuttelaars [9] describes the sea bed evolution in a single inlet system. This is done in a width- and depth-averaged model. With these assumptions the sea bed in equilibrium can be computed analytically. However because of the averaging with respect to the depth, the dynamics of the water velocity and sediment transport in the vertical direction can only be included parametrically. This is due to the fact that the erosion of the sea bed and deposition of sediment depends for a large part on the water velocity at the sea bed which has to be linked to the velocity averaged over the depth. To take the vertical dynamics better in account, ter Brake [11] included a new parametrisation of the sediment depositions to capture the vertical dynamical behaviour as good as possible. However, it is not possible to obtain analytical equilibrium solutions to the equation of the sea bed evolution any more.

On the subject of double inlet systems the research conducted is very sparse. Early research on the stability and existence of equilibrium solutions in double inlets system is presented in van de Kreeke, [12]. In this article only the evolution of the cross-sectional areas of the inlets was modelled for the inlet systems. Similar research on depth-averaged hydrodynamical was done in Brouwer et al. [2], where the stability of double inlet systems was investigated allowing for spatially varying hydrodynamics in the back barrier.

Finally, research on morphodynamical models in a double inlet system has been recently conducted in Xiao et al. [4], which uses a cross-sectionally averaged model to analyse the sea bed evolution to find equilibrium solutions in double inlet systems taking both the inlets and the back barrier basins as morphodynamically active. In this model the water velocity and sediment concentration on the vertical coordinate is not taken into account.

1.2 Research questions

The overview reveals a clear gap in knowledge: morphodynamics in 2DV-models, in other words models that include processes in the vertical direction. No research has been conducted on both single and double inlets. This raised the following questions:

1. It is possible to construct a 2DV morphodynamical model incorporating sea bed evolution to find equilibrium solutions of the sea bed?
2. How do morphodynamical behaviour and equilibrium solutions in a 2DV-model compare to those of a one-dimensional width and depth-averaged model?
3. Is it possible for an inlet system to have multiple equilibrium solutions?

To answer these questions an exploratory 2DV morphodynamical model is constructed. This model will be highly simplified to quantify the effects of not averaging the vertical direction of the domain. This model is obtained by scaling the equations. Next an asymptotic expansion is used to solve the most important balances in the equations.
This model will focus on morphodynamical behaviour, thus using the change in sea bed in one semi-diurnal tide cycle to update the sea bed. The hypothesis is that this method will eventually lead to an equilibrium solution. This is discussed in chapter 2 of this article. The outcome of this will answer research question 1.
Because all governing equations are non-linear, numerical schemes are used to solve them. As a compromise between speed and accuracy second order accurate schemes are used to compute the solutions.

Research questions 2 and 3 are addressed in chapter 3. First of all, solutions to the morphodynamical model discussed in chapter 2 are compared to solutions found in 1-dimensional depth-averaged morphodynamical models. This comparison strives to find the impact of including the depth of the domain into the equilibrium solutions found and will give an answer to research question 2.
Also in chapter 3, parameter sensitivity is performed to asses the importance of

the single parameters defining the domain of computation. Furthermore, it is investigated for which set of parameters multiple equilibrium solutions exist.

Chapter 2

The mathematical model

This section describes the mathematical model that is developed to compute the sea bed evolution in double inlet systems. This type of model can also be used for single inlet systems but the formulation of the boundary conditions are slightly more complex and will not be discussed in this thesis.

Firstly, the characteristics of the domain will be discussed. Then, the governing equations in the domain are discussed. The parameter values describing the system are defined in Table 2.1. The values of these parameters are obtained from observations.

Next, two methods for finding equilibrium solutions are presented. The first method is to directly find a sea bed for which there is no temporal change in sea bed and the second method is to iteratively update the sea bed using a time-integration approach until the sea bed converges to an equilibrium solution.

Table 2.1: Table showing magnitude of important parameters

Parameter	Symbol	Dimension	Magnitude
Semi-diurnal angular tide frequency	σ	s^{-1}	$1.4 \cdot 10^{-4}$
Length of the inlet system	L	km	20
Height of the water column	H	m	10
Typical density of the water	ρ_0	kgm^{-3}	1020
Amplitude of the semidiurnal tide	M_2	m	1.35
Phase difference of semidiurnal tide between two ends of double inlet system	ϕ	degrees	20
Vertical eddy viscocity	A_v	m^2s^{-1}	0.012
Partial slip friction parameter	s	ms^{-1}	0.049

Figure 2.1: Top view of the domain

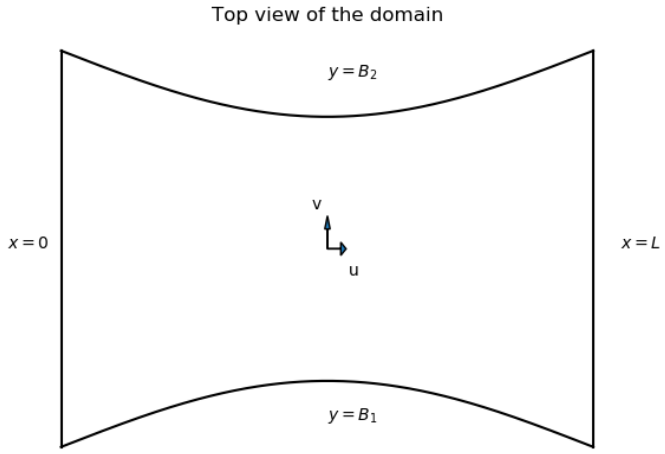

Figure 2.2: Side view of the domain

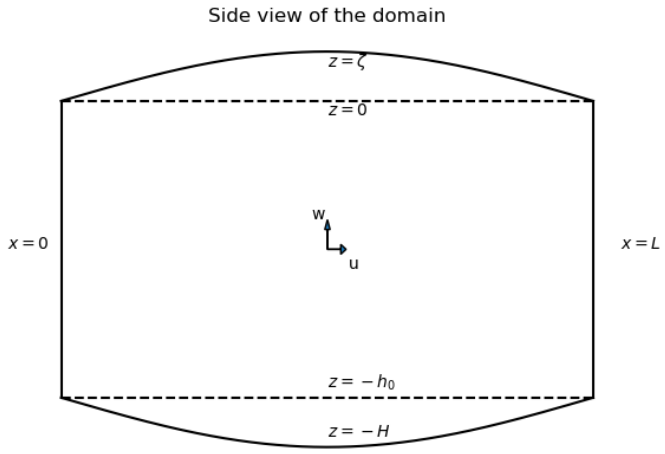

2.1 Geometry

In Figures 2.1 and 2.2 the geometry of a double inlet system is shown, with Figure 1 the top view and Figure 2 the side view respectively. The top view shows that the inlet system is connected to the outer sea at $x = 0$ and $x = L$ which are straight lines, where its width is confined by two shorelines B_1 and B_2 which are not necessarily straight lines, and can vary along the length of the inlet system.
From the side view it can be seen that the domain is bounded at the top by a free surface elevation $z = \zeta$ and at the bottom by the undisturbed water depth $z = -H$. Both the free surface elevation ζ and the undisturbed water depth H are dependent on the longitudinal coordinate x.

The length of the domain is constant and defined by L. The width of the domain is given by $B = B_2 - B_1$ and the water depth by $h = H + \zeta$.

2.2 Morphodynamic Model

A morphodynamical model describes the evolution of the bottom due to erosion and deposition of sediment. The main initiator to this evolution of the bottom is tidal motion, because this tidal motion results in stresses exerted at the bed. Due to these stresses, sediment is suspended in the water column and transported by advective and diffusive processes. Next, due to the weight of the sediment it will sink to the bottom again, resulting in bed changes.

This difference in erosion of the sea bed and deposition of sediment on the sea bed results in the evolution of the bed. From observations it is found that typical changes in the water motion are much faster than those of the bottom. Because of this, two time scales can be introduced which characterise these changes, a short time-scale t for changes in water motion and a long time-scale τ for changes in the sea bed. The short time-scale is related to the semi-diurnal tidal cycle which characterizes the change in water motion; the sea bed H is assumed to be constant during such a tidal cycle.

To capture the bed evolution the sediment, deposition and erosion have to be calculated. For this some modules are needed:

1. the hydrodynamical module: this includes the water velocity in all directions u, v and w, and the free water surface elevation ζ,
2. the suspended sediment module that results in the suspended sediment concentration c,
3. the bed evolution module that updates the location of the sea bed z_b.

2.2.1 Water motion

In this section the method to compute the water motion, consisting of the free surface elevation and the water velocity, in a double inlet is described. This will result in the leading order hydrodynamics equation. A more detailed approach is found in the appendix. In physics and mathematics, the motion of viscous fluids is described by a set of partial differential equations known as the Navier-Stokes equations [6]:

$$\frac{\partial \rho}{\partial t} + \frac{\partial \rho u}{\partial x} + \frac{\partial \rho v}{\partial y} + \frac{\partial \rho w}{\partial z} = 0, \tag{2.1a}$$

$$\frac{\partial \rho u}{\partial t} + \frac{\partial \rho u^2}{\partial x} + \frac{\partial \rho uv}{\partial y} + \frac{\partial \rho uw}{\partial z} = \rho b_x + \frac{\partial \sigma_{xx}}{\partial x} + \frac{\partial \sigma_{xy}}{\partial y} + \frac{\partial \sigma_{xz}}{\partial z}, \tag{2.1b}$$

$$\frac{\partial \rho v}{\partial t} + \frac{\partial \rho uv}{\partial x} + \frac{\partial \rho v^2}{\partial y} + \frac{\partial \rho vw}{\partial z} = \rho b_y + \frac{\partial \sigma_{xy}}{\partial x} + \frac{\partial \sigma_{yy}}{\partial y} + \frac{\partial \sigma_{yz}}{\partial z}, \tag{2.1c}$$

$$\frac{\partial \rho w}{\partial t} + \frac{\partial \rho uw}{\partial x} + \frac{\partial \rho vw}{\partial y} + \frac{\partial \rho w^2}{\partial z} = \rho b_z + \frac{\partial \sigma_{xz}}{\partial x} + \frac{\partial \sigma_{yz}}{\partial y} + \frac{\partial \sigma_{zz}}{\partial z}, \tag{2.1d}$$

with ρ the density, u, v and w the fluid velocity in respectively the x, y and z direction, b_i the outside body forces on the fluid in the i-direction and σ_{ij} the stress tensor. Eq. (2.1a) is known as the continuity equation and equations (2.1b), (2.1c) and (2.1d) as the momentum equations.

The body forces b_i are defined by the acceleration due to gravity and other forces like the Coriolis force. The stress tensor σ_{ij} can be rewritten as $\sigma_{ij} = -p\delta_{ij} + \tau_{ij}$ with δ_{ij} the unity tensor and τ the shear stress tensor. The turbulent shear stress τ is then related to the velocity gradient via a closure scheme [8], giving:

$$\tau_{xx} = 2\rho A_h \frac{\partial u}{\partial x}, \quad \tau_{xy} = \tau_{yx} = \rho A_h \left(\frac{\partial u}{\partial y} + \frac{\partial v}{\partial x} \right), \tag{2.2a}$$

$$\tau_{yy} = 2\rho A_h \frac{\partial v}{\partial y}, \quad \tau_{xz} = \tau_{zx} = \rho \left(A_v \frac{\partial u}{\partial z} + A_h \frac{\partial w}{\partial x} \right), \tag{2.2b}$$

$$\tau_{zz} = 2\rho A_v \frac{\partial w}{\partial z}, \quad \tau_{yz} = \tau_{zy} = \rho \left(A_v \frac{\partial v}{\partial z} + A_h \frac{\partial w}{\partial y} \right). \tag{2.2c}$$

To solve these equations boundary conditions have to be imposed. First, at the bottom, denoted by $z = -H$, no fluid can leave the domain, thus a no normal flow boundary condition applies. Assuming the bottom to fixed in time, one finds:

$$u \frac{\partial H}{\partial x} + v \frac{\partial H}{\partial y} + w = 0. \tag{2.3}$$

The same type of boundary condition is imposed at the free surface elevation $z = \zeta$:

$$\frac{\partial \zeta}{\partial t} + u \frac{\partial \zeta}{\partial x} + v \frac{\partial \zeta}{\partial y} - w = 0. \tag{2.4}$$

The shear stresses τ_s and τ_b receptively at the bottom $z = -H$ and the free surface elevation $z = \zeta$ can be expressed in terms of the normally directed stresses in each direction:

$$\tau_s = -\tau_{xx}\frac{\partial \zeta}{\partial x} - \tau_{xy}\frac{\partial \zeta}{\partial y} + \tau_{xz}, \tag{2.5a}$$

$$\tau_b = \tau_{xx}\frac{\partial H}{\partial x} + \tau_{xy}\frac{\partial H}{\partial y} + \tau_{xz}. \tag{2.5b}$$

Apart from the boundary conditions (2.3) and (2.4), a second condition has to be imposed; such as a free slip, no slip or partial slip condition. In this thesis for the free surface elevation a free slip condition is imposed:

$$A_v\frac{\partial u}{\partial z} = 0 \quad \text{at } z = \zeta,$$

and for the bottom a partial slip condition is used:

$$A_v\frac{\partial u}{\partial z} = su \quad \text{at } z = -H,$$

where s is the partial slip parameter.

The type of systems considered in this thesis are shallow. Because of this, by scaling the vertical momentum equation (2.1d) it is found that an approximate balance exists between the terms ρb_z and $\frac{\partial \sigma_{zz}}{\partial z}$, where the latter term is well-approximated as $\frac{\partial \sigma_{zz}}{\partial z} = -\frac{\partial p}{\partial z}$. Therefore, all other terms from the equation can be removed.
Assuming incompressibility, using the Boussinesq approximation and assuming the density of the water is equal throughout the domain, the resulting shallow water equations read:

$$\frac{\partial u}{\partial x} + \frac{\partial v}{\partial y} + \frac{\partial w}{\partial z} = 0, \tag{2.6a}$$

$$\frac{\partial u}{\partial t} + u\frac{\partial u}{\partial x} + v\frac{\partial u}{\partial y} + w\frac{\partial u}{\partial z} = -\frac{1}{\rho}\frac{\partial p}{\partial x} + \frac{\partial}{\partial x}\left(A_h\frac{\partial u}{\partial x}\right) + \frac{\partial}{\partial y}\left(A_h\frac{\partial u}{\partial y}\right) + \frac{\partial}{\partial z}\left(A_v\frac{\partial u}{\partial z}\right), \tag{2.6b}$$

$$\frac{\partial v}{\partial t} + u\frac{\partial v}{\partial x} + v\frac{\partial v}{\partial y} + w\frac{\partial v}{\partial z} = -\frac{1}{\rho}\frac{\partial p}{\partial y} + \frac{\partial}{\partial x}\left(A_h\frac{\partial v}{\partial x}\right) + \frac{\partial}{\partial y}\left(A_h\frac{\partial v}{\partial y}\right) + \frac{\partial}{\partial z}\left(A_v\frac{\partial v}{\partial z}\right), \tag{2.6c}$$

$$\frac{\partial p}{\partial z} = -\rho g. \tag{2.6d}$$

In deriving these expressions, the effects of the Coriolis forces have been neglected. The vertical and horizontal eddy viscosity denoted by A_v and A_h are used to model the turbulence in both directions, parametrising the mixing by effects of small scale turbulent motion. Furthermore, g is the gravitational acceleration.

Eq. (A.1d) can be solved to give $p = p_a + \rho g(\zeta - z)$, with the pressure at the free surface elevation ζ equal to the atmospheric pressure p_a.

To focus on the hydrodynamics in the x and z direction the equations are averaged over the width, resulting in:

$$\frac{\partial \hat{u}}{\partial x} + \frac{\partial \hat{w}}{\partial z} + \frac{1}{B_2 - B_1}\frac{\partial (B_2 - B_1)}{\partial x}\hat{u} = 0, \tag{2.7a}$$

$$\frac{\partial \hat{u}}{\partial t} + \frac{\partial \hat{u}^2}{\partial x} + \frac{\partial (\hat{u}\hat{w})}{\partial z} = g\frac{\partial \hat{\zeta}}{\partial x} + \hat{A}_v \frac{\partial^2 \hat{u}}{\partial z^2}. \tag{2.7b}$$

With the assumption that in a straight channel the water motion in the y-direction v is equal to zero and scaling all terms in equation (A.1c) can be removed thus this equation can be removed in its entirety. Physical quantities in equations (2.7a) and (2.7b) with a overhead tilde are width averaged. Furthermore, the vertical eddy viscosity $\hat{A}_v$ is assumed to be constant. Note that both terms with A_h are neglected as they are much smaller than the other terms.

The boundary conditions are width-averaged in the same way and give:

$$\hat{u}\frac{\partial H}{\partial x} + \hat{w} = 0 \quad \text{at } z = -H, \tag{2.8a}$$

$$\frac{\partial \hat{\zeta}}{\partial t} + \hat{u}\frac{\partial \hat{\zeta}}{\partial x} - \hat{w} = 0 \quad \text{at } z = \hat{\zeta}. \tag{2.8b}$$

The shear stresses and the slip boundary conditions can be used to define the boundary conditions:

$$s\hat{u} = A_v \frac{\partial \hat{u}}{\partial z} \quad \text{at } z = -H, \tag{2.9a}$$

$$A_v \frac{\partial \hat{u}}{\partial z} = 0 \quad \text{at } z = \zeta. \tag{2.9b}$$

The next step is to make the equations non-dimensional and finding the main balance between the terms in the individual equations. This leads to:

$$\frac{\partial \hat{u}}{\partial x} + \frac{\partial \hat{w}}{\partial z} + \frac{1}{B_2 - B_1}\frac{\partial (B_2 - B_1)}{\partial x}\hat{u} = 0 \tag{2.10a}$$

$$\frac{\partial \hat{u}}{\partial t} + \varepsilon\frac{\partial \hat{u}^2}{\partial x} + \varepsilon\frac{\partial (\hat{u}\hat{w})}{\partial z} = \frac{\partial \hat{\zeta}}{\partial x} + \frac{\partial^2 \hat{u}}{\partial z^2}, \tag{2.10b}$$

with ε a small parameter defined as $\varepsilon = \frac{U}{\sigma L}$. A detailed derivation can be found in the appendix.
To solve these equations an asymptotic expansion of $\hat{u}, \hat{w}$ and $\hat{\zeta}$ is defined:

- $\hat{u} = \mathbb{R}\left[(u^0(x,z) + \varepsilon u^1(x,z) + \ldots)e^{i\sigma t}\right]$,
- $\hat{w} = \mathbb{R}\left[(w^0(x,z) + \varepsilon w^1(x,z) + \ldots)e^{i\sigma t}\right]$,

- $\hat{\zeta} = \mathbb{R}\left[(\zeta^0(x) + \varepsilon\zeta^1(x) + \ldots)e^{i\sigma t}\right]$,

The asymptotic expansions are introduced into equations (2.10a) and (2.10b), and the resulting equations are ordered depending on this small parameter. Retaining only the leading order terms the following width-averaged shallow water equations are obtained:

$$\frac{\partial u^0}{\partial x} + \frac{\partial w^0}{\partial z} + \frac{1}{B_2 - B_1}\frac{\partial (B_2 - B_1)}{\partial x}u^0 = 0, \tag{2.11a}$$

$$i\sigma u^0 - g\frac{\partial \zeta^0}{\partial x} + A_v\frac{\partial^2 u^0}{\partial z^2} = 0, \tag{2.11b}$$

The boundary conditions at the free surface are rewritten as equivalent boundary conditions at $z = 0$, using a Taylor expansion around $z = 0$:

$$u^0\frac{\partial H}{\partial x} = -w^0 \quad \text{at } z = -H, \tag{2.12a}$$

$$\frac{\partial \zeta^0}{\partial t} = w^0 \quad \text{at } z = 0. \tag{2.12b}$$

On the sea bed the boundary conditions read:

$$w^0(x, -H) = -u^0\frac{\partial H}{\partial x}, \tag{2.13a}$$

$$A_v\frac{\partial u^0}{\partial z} = su^0. \tag{2.13b}$$

To solve for u^0, w^0 and ζ^0, first Eq. (A.10b) is solved for u^0. This results in

$$u^0(x, z) = -\frac{g}{i\sigma}\frac{\partial \zeta^0}{\partial x}\left(1 - \frac{s\cosh(\beta z)}{A_v\beta\sinh(\beta H) + s\cosh(\beta H)}\right), \tag{2.14}$$

with $\beta = \sqrt{\frac{i\sigma}{A_v}}$. Substituting this expression for u^0 in Eq. (A.10a), and integrating this equation over the depth, leads to a differential equation for ζ^0:

$$\frac{\partial^2 \zeta^0}{\partial x^2} + \frac{1}{B_2 - B_1}\frac{\partial (B_2 - B_1)}{\partial x}\frac{\partial \zeta^0}{\partial x} - \frac{\sigma^2}{g\gamma}\zeta^0 = 0, \tag{2.15}$$

where γ is defined by

$$\gamma = \frac{s\sinh\beta H}{A_v\beta^2\sinh\beta H + s\beta\cosh\beta H} - H$$

If $\gamma(x)$ and $\frac{1}{B_2 - B_1}\frac{\partial (B_2 - B_1)}{\partial x}$ both are constant in space, an analytical solution can be obtained, otherwise a numerical scheme has to be used to solve Eq. (A.14).

The free surface elevation ζ^0 is prescribed at the seaward sides of the double inlet system as equal to their respective value at the seas. In this thesis only

the M_2 tidal constituent will be considered. Hence, at the first inlet the sea surface elevation reads:

$$\zeta^0(0,t) = A^I_{M_2} \cos(\sigma t),$$

with $A^I_{M_2}$ the tidal amplitude at inlet I and σ the M_2 tidal frequency. The free surface elevation at the other inlet II, located at $x = L$, of the inlet system is defined as

$$\zeta^0(L,t) = A^{II}_{M_2} \cos(\sigma t - \phi_{M_2}).$$

Because there is a spatial difference between both entrances usually there is a phase difference and an amplitude difference between the sea levels at inlets I and II. In this thesis it is assumed that the amplitudes of the semi-diurnal tide at both entrances are equal, in other words: $A^I_{M_2} = A^{II}_{M_2}$, the phase difference is denoted by φ_{M_2}.

2.2.2 Sediment concentration

The next step in calculating the evolution of a sea bed is the calculation of the sediment concentration in the inlet system. This step is needed as the erosion and deposition of sediment, which determine the sea bed evolution, both are dependent on the sediment concentration. To derive an equation to compute the sediment concentration, conservation of mass is used:

$$\frac{\partial c}{\partial t} + \overrightarrow{\nabla} \cdot \overrightarrow{F} = 0,$$

where $\overrightarrow{F}$ is the total sediment concentration flux in the inlet system and c is the suspended sediment concentration. The sediment flux consists of three contributions: advective, diffusive and settling flux. They are respectively defined by:

$$F_a = c\overrightarrow{u} + cwe_z,$$

$$F_d = -K_h \nabla c - K_v \frac{\partial c}{\partial z} e_z,$$

$$F_s = -cw_s e_z.$$

Where $\overrightarrow{u}$ is the 3-dimensional water velocity, e_z the unit vector in the z-direction and K_h and K_v the horizontal and vertical eddy diffusivity coefficient, respectively. Furthermore, w_s is the settling velocity. This leads to the following partial differential equation:

$$\frac{\partial c}{\partial t} + \frac{\partial (uc)}{\partial x} + \frac{\partial (vc)}{\partial y} + \frac{\partial (c(w - w_s))}{\partial z} = \frac{\partial (K_h c_x)}{\partial x} + \frac{\partial (K_h c_y)}{\partial y} + \frac{\partial (K_v c_z)}{\partial z}. \quad (2.16)$$

Like the derived water motion equations this is a complex partial differential equation and very difficult to solve. Thus, averaging, nondimensionalization and collecting only the leading order terms is used to simplify the equation.

By width-averaging and scaling Eq. (2.16) the following dimensionless equation is derived:

$$\frac{\partial \hat{c}}{\partial t} + \varepsilon \left(\hat{u}\frac{\partial \hat{c}}{\partial x} + \hat{w}\frac{\partial \hat{c}}{\partial z} \right) - w_s^* \frac{\partial \hat{c}}{\partial z} - \varepsilon \frac{\partial^2 \hat{c}}{\partial x^2} - K_h^* \frac{\partial^2 \hat{c}}{\partial z^2} = 0. \tag{2.17}$$

Parameters with an asterisk are nondimensional in this equation. With the asymptotic expansion $\hat{c} = c^0 + \varepsilon c^1 + O(\varepsilon^2)$, keeping leading order terms, the following the main dimensionful balance is obtained:

$$\frac{\partial c^0}{\partial t} - w_s \frac{\partial c^0}{\partial z} - K_v \frac{\partial^2 c^0}{\partial z^2} = 0 \tag{2.18}$$

This equation only contains derivatives in the vertical direction. Two boundary conditions at $z = 0$ and $z = -H$ are needed to be solve Eq. (2.18).
As the free surface elevation does not allow sediment to leave the system we impose a no flux condition at $z = \zeta$:

$$w_s c^0 + K_v \frac{\partial c^0}{\partial z} = 0. \tag{2.19}$$

At the bottom the sediment flux is related to the erosion and deposition fluxes of sediment:

$$E_s = \quad -K_h \frac{\partial c}{\partial x} n_x - K_v \frac{\partial c}{\partial z} n_z = w_s c^* = w_s \rho_s a \frac{|\tau_b(t,x)|}{\rho_0 g' d_s}, \tag{2.20a}$$

$$D = \quad w_s c n_z. \tag{2.20b}$$

In this expression n_x and n_z define the components of the normally directed unit vector at the bottom in the x and z-direction respectively. For the sediment concentration at the sea bed $z = -H$ a reference concentration c^* is used [3, 5]. Furthermore, ρ_s is the sediment density, g' the reduced gravity, a the erosion coefficient and d_s the grain size. The forcing term in this expression $\tau_b(t,x)$ is the bed shear stress causes by the velocity of the water. The erosion coefficient models the along-channel distribution of easily erodible sediment. It can be expressed due to partial slip condition Eq. (2.13b) at the sea bed with:

$$\tau_b = \rho_0 K_v \frac{\partial u^0}{\partial z} = \rho s u^0.$$

The vertical eddy viscosity parameter A_v is assumed to be equal to the eddy diffusity parameter K_v. Because the bottom H does not depend on z the normally directed component n_z is equal to 1. Substituting asymptotic expansions for u and c into Eq. (A.32) and retaining only leading order terms gives boundary condition:

$$-K_v \frac{\partial c^0}{\partial z}\Big|_{z=-H} = w_s \rho_s a \frac{s|u^0(t,-H)|}{\rho_0 g' d_s}.$$

Since the leading order constituent of the water velocity u^0 only consists of an M_2 tidal constituent, the absolute value of u^0 will consist of a residual contribution and even overtides. Since we focus on the morphodynamic evolution,

driven by diffusive processes, it turns out that only the residual component is needed. The residual part needed to determine the concentration, is obtained by:

$$a_0 = \int_0^T |u^0 e^{i\sigma t}| \mathrm{d}t.$$

Finally, the bottom boundary condition becomes:

$$-K_v \frac{\partial c^0}{\partial z}(t, -H) = w_s \rho_s a \frac{s a_0(x)}{g' d_s}.$$

Because only the residual contribution a^0 is forcing the differential equation, the solution will only consist of the residual component c^{00} of the leading order sediment concentration c^0. This residual term c^{00} does not depend on time, thus the leading order differential equation for the concentration can be rewritten as:

$$w_s \frac{\partial c^{00}}{\partial z} + K_v \frac{\partial^2 c^{00}}{\partial z^2} = 0, \tag{2.21}$$

which, together with the appropriate boundary condition, results in the following solution:

$$c^{00}(x, z) = \frac{a \rho_s s a_0}{g' d_s} \exp\left(-\frac{w_s (H + z)}{K_v}\right). \tag{2.22}$$

In this expression, the dependency of c^{00} on the longitudinal coordinate x is hidden in a_0, the tidally averaged absolute M_2 velocity and H, the undisturbed water depth.

2.2.3 Sea bed evolution

The last governing equation in this model is the sea bed evolution equation. This equation describes the sea bed evolution due to the erosion of the sea bed and the deposition of sediment. If more sediment is deposited than eroded the sea bed will increase compared to the height of the initial sea bed.

It is assumed that the sea bed does not change significantly during a semi-diurnal tide cycle. This means that the sea bed evolution equation does not depend on the short time scale t associated with the semi-diurnal tide cycle but only on the long time scale τ. This gives the following equation for the sea bed evolution [13]:

$$\rho_s (1 - p) \frac{\partial z_b}{\partial \tau} = D - E_s,$$

where p is the porosity of the sediment and z_b the height of the seabed measured from a reference level. Furthermore, E_s is the erosion of the seabed and D the deposition of sediment.

In this model it is assumed that the dynamics in the inlet system does not

influence the sea bed at the inlets. To achieve this the sea bed at the inlets has to be fixed, requiring an extra diffusion contribution to be added:

$$\rho_s(1-p)\frac{\partial z_b}{\partial \tau} + \lambda \frac{\partial^2 z_b}{\partial x^2} = D - E_s.$$

This diffusion models the tendency of sediment to roll downhill. This addition allows the sea bed to stay constant at $x = 0$ and $x = L$, which is captured by the boundary conditions:

$$z_b(0) = 0,$$
$$z_b(L) = 0.$$

The magnitude of λ is assumed to be $\lambda = 2 \cdot 10^{-4}$ [9].

Now $D - E_s$ has to expressed in terms of c^{00}. By integrating $D - E_s$ over the width and depth, this can be expressed by:

$$(B_2-B_1)(-D+E_s) = \frac{\partial}{\partial t}\int_{-H}^{\zeta}(B_2-B_1)\hat{c}\mathrm{d}z + \frac{\partial}{\partial x}\int_{-H}^{\zeta}(B_2-B_1)\hat{u}\hat{c}\mathrm{d}z - \frac{\partial}{\partial x}\int_{-H}^{\zeta}(B_2-B_1)K_h\frac{\partial \hat{c}}{\partial x}\mathrm{d}z, \tag{2.23}$$

with B_2 and B_1 the functions describing the shores of the inlet system. The expression $(B_2-B_1)\hat{u}\hat{c}$ is of order $O(\varepsilon)$ and denotes the advective hydrodynamic behaviour which is not in the focus of this research thus will not be included. Now averaging over a tidal period, substituting c and u with their respective asymptotic expansions and Taylor expanding border $z = \zeta$ the leading order expression becomes:

$$(B_2 - B_1)(-D + E_s) = -\frac{\partial}{\partial x}\int_{-H}^{0}(B_2 - B_1)K_h\frac{\partial c^{00}}{\partial x}\mathrm{d}z. \tag{2.24}$$

Because Eq. (2.24) is tidally averaged the term $\int_{-H}^{0}(B_2 - B_1)c^{00}$ does not depend on the short time scale t.
This relation between erosion of the sea bed and deposition of sediment can now be substituted into the sea bed evolution equation to give:

$$(B_2 - B_1)\rho_s(1-p)\frac{\partial z_b}{\partial \tau} + \lambda\frac{\partial^2 z_b}{\partial x^2} = \frac{\partial}{\partial x}\int_{-H}^{0}(B_2 - B_1)K_h\frac{\partial c^{00}}{\partial x}\mathrm{d}z. \tag{2.25}$$

The right hand side of this expression is implicitly dependent on the sea bed z_b. Thus, when iteratively computing the sea bed evolution, the sea bed z_b has to be updated in order to compute it.

2.3 Solution methods

Alternatively, a hybrid method is possible to ensure the best accuracy.

With all governing equations in place, a method to compute an equilibrium is the next step. To obtain ζ^0 and z_b, a numerical scheme is used, using the same grid for all variables.
To achieve numerical stability an implicit numerical method is preferred over an explicit method but note that the right hand side of expression (2.25) can not be solved implicitly because it is an non-linear term.
Let N be the number of grid points in the x-direction. The number of time steps can not be determined a posteriori as it is uncertain when an equilibrium will be achieved.

For this a threshold value TOL is introduced that determines if an equilibrium is achieved. If $||z_b||_2 \leq TOL$ it can be assumed that the system is in equilibrium. A good choice for this value is $TOL = 10^{-10}$.

To arrive at such an equilibrium two methods can be used: minimization of the sea bed evolution term or iterations over the sea bed evolution.
Note that the change in sea bed is determined by the difference in erosion and deposition. Thus, if a sea bed H_{min} can be found that minimizes this difference such that $||z_b||_2 \leq TOL$, an equilibrium is found.

An alternative way is to start with an arbitrary bed profile $H(x)$ and iteratively update the sea bed with the computed difference between erosion and deposition and use the long time scale to converge to an equilibrium. Because the bed changes are small, this process can be time consuming.

Lastly, a hybrid between these two methods can also be employed. First assume a minimizing sea bed up to a larger tolerance and start the iteration from this minimized sea bed. Starting closer to the equilibrium solution does reduce the computation time and the fact that a minimizing sea bed is used it is almost certain that the time integrator converges to an equilibrium.

2.3.1 Minimization

From the equation for sea bed evolution it follows that the sea bed will not change if

$$M(H) = \left(\frac{\partial}{\partial x} \int_{-H}^{0} (B_2 - B_1) K_h \frac{\partial c^{00}(H)}{\partial x} \mathrm{d}z - \lambda \frac{\partial^2 H}{\partial x^2} \right)^2$$

is equal to zero for all locations in the system. On the long time scale this expression is only dependent on the sea bed H, thus by finding an H for which M is equal to zero will give an equilibrium.
Because of the fact that H is defined on N grid points this gives N degrees of freedom, thus N coefficients have to be minimized. As most unconstrained nonlinear minimization methods are of order $O(N^2)$ this is not feasible in reasonable time.

A different approach would be to minimize over $\int_0^L M(H)\mathrm{d}x$. This way only a single value has to be minimized but the N degrees of freedom is implicitly hidden in this value. Thus obtaining a true root is impossible.

Instead, the threshold parameter TOL is used and a function space over which to minimize $M(H)$ is defined.

All minimizing sea bed are constrained by the fact that $H_{min}(0) = H_{min}(L) = 0$. All functions in the function space $C(\mathbb{R})$ which conform to these constraints can be constructed by a set of basis functions defined as:

$$V := \left\{ x \mapsto d_i \sin\left(\frac{i\pi x}{L}\right) : i \in \mathbb{N}, d_i \in \mathbb{R} \right\},$$

with the minimizing sea bed defined as:

$$H_{min} = \sum_{i=1}^{n} d_i \sin\left(\frac{i\pi x}{L}\right),$$

with n the number of modes such that $|M(H_{min})| \leq TOL$.

A numerical optimization scheme which can be used for this routine is the Broydon-Fletcher-Goldfarb-Shanno algorithm. It uses approximations to the Hessian matrices of M with a generalized secant method. The secant method is an iterative root-finding algorithm and approximates the roots of M. In contrast to the better known Newton-Raphson method this algorithm is of order $O(n^2)$ instead of $O(n^3)$ which should yield shorter computation times. When increasing n the approximation of the equilibrium will improve.
The number of modes n to find a minimum such that $|M(H)| \leq TOL$ is much smaller than the number of grid points N, thus this method is much smaller than finding a sea bed H such that $M(H)$ is equal to zero for all grid point.

2.3.2 Iterative method

The second method of finding an equilibrium solution is to iteratively update the sea bed until

$$||\Delta z_b||_2 \leq TOL,$$

with $\Delta z_b = z_b^{i+1} - z_b^i$, z_b^i being the sea bed at iteration step i. With this method, the initial sea bed can be chosen $H(\tau = 0) = H(x)$. Then the sea at iteration j is:

$$H_j = h_0 + \sum_{i=0}^{j-1} z_b^i.$$

Figure (2.3) shows the iterative method in the form of a flowchart.

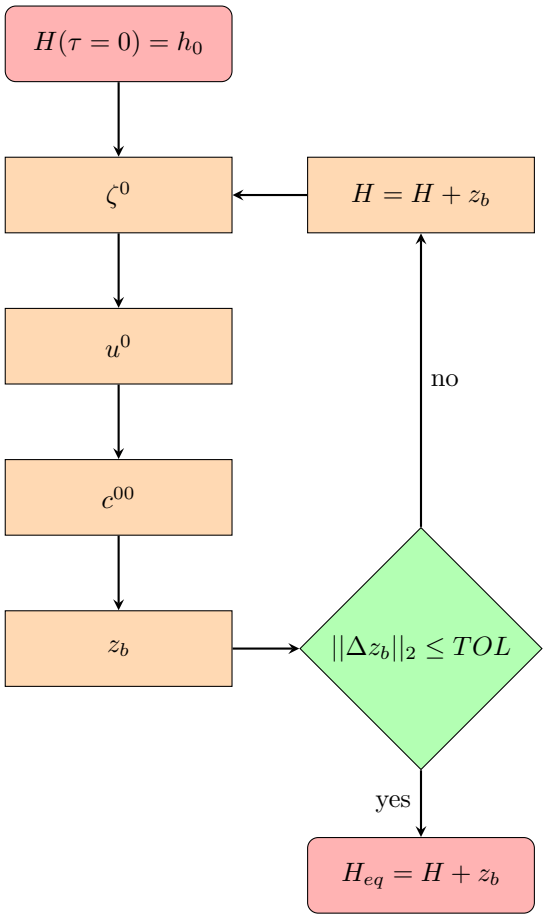

Figure 2.3: Flow chart displaying the process in the iterative method

2.3.3 Hybrid method

Two different methods of finding equilibrium solutions have been discussed in the previous sections. Both methods use different routines but this does not mean that they cannot be combined.
The problem with the minimization routine is that a rough estimate of the equilibrium can be found easily for around 10 modes, but converging to an accurate equilibrium solution requires at least 100 or more modes to be included in the minimizing sea bed. This is very slow. On the other hand, the sea bed evolution method converges to an equilibrium solution but very slowly when using an arbitrary initial condition.

Because of this, using both methods in combination is a good method to find equilibria in shorter computation time.
The first step is to find a minimizing sea bed using approximately 10 modes, and then apply the sea bed evolution time integrator starting from this sea bed.

This also has the added benefit that with the minimization method it is possible to find multiple equilibrium solutions. Finding local minimizing sea beds instead of global minimizing sea beds can be used for this.

2.4 Depth-averaged version

With the construction of the mathematical model with governing equations and the two solution methods equilibrium solutions now can be found. The next step is to investigate how the solutions to this 2DV-model relate to solutions found in width and depth-averaged models, i.e. one-dimensional models.
One of the problems in depth-averaged model is that the erosion of sediment from the sea bed can not be directly expressed in terms of the velocity at the sea bed. This is because, by averaging over the depth, the dependence of u on the z-direction has been removed, only the depth averaged velocity is known.

2.4.1 Conversion factor

A common way to circumvent this problem is to define a typical parameter U that defines the relation between $u^0(x, z = -H)$ at the sea bed and the depth averaged $\hat{u}^0(x)$. This characteristic U is initially defined and usually does not change during sea bed evolution. However, during the sea bed evolution the sea bed changes in such a way that this characteristic U does not represent the relation between $u^0(x, z = -H)$ and $\hat{u}^0(x)$ any more. Depending on the change in sea bed, this characteristic U has to be updated to give reliable results. From

averaging the 2DV horizontal velocity over the depth this can easily be done:

$$\hat{u}^0(x) = \int_{-H}^{0} u^0 \mathrm{d}z = \int_{-H}^{0} -\frac{g}{i\sigma}\frac{\partial \zeta^0}{\partial x}\left(1 - \frac{s\cosh(\beta z)}{A_v\beta\sinh(\beta H) + s\cosh(\beta H)}\right)\mathrm{d}z$$

$$= -\frac{g}{i\sigma}\frac{\partial \zeta^0}{\partial x}\left[1 - \frac{s\sinh(\beta z)}{\beta H(A_v\beta\sinh(\beta H) + s\cosh(\beta H))}\right].$$

The water velocity at the sea bed is given by:

$$u^0(x,-H) = -\frac{g}{i\sigma}\frac{\partial \zeta^0}{\partial x}\left(1 - \frac{s\cosh(\beta H)}{A_v\beta\sinh(\beta H) + s\cosh(\beta H)}\right).$$

With these expressions the water velocity at the sea bed can be expressed in terms of depth-averaged water velocity:

$$u^0(x,-H) = \left[\frac{1 - \frac{s\cosh(\beta H)}{A_v\beta\sinh(\beta H)+s\cosh(\beta H)}}{1 - \frac{s\sinh(\beta H)}{\beta H(A_v\beta\sinh(\beta H)+s\cosh(\beta H))}}\right]\hat{u}^0(x).$$

Therefore, instead of using a characteristic U the conversion factor F_{conv} can be used in depth-averaged models:

$$F_{conv} = \frac{1 - \frac{s\cosh(\beta H)}{A_v\beta\sinh(\beta H)+s\cosh(\beta H)}}{1 - \frac{s\sinh(\beta H)}{\beta H(A_v\beta\sinh(\beta H)+s\cosh(\beta H))}}$$

2.4.2 Depth-averaged model

A depth-averaged morphodynamical model for double inlets is defined in [10]. This model also consists of four governing equations:

$$\frac{i\sigma g H^2}{i\sigma H + r}\frac{\partial^2 \zeta}{\partial x^2} + \left(\frac{\partial}{\partial x}\left[\frac{i\sigma g H^2}{i\sigma H + r}\right]\right)\frac{\partial \zeta}{\partial x} + \sigma^2\zeta = 0,$$

$$u = -\frac{g}{i\sigma + \frac{r}{H}}\frac{\partial \zeta}{\partial x},$$

$$K_h\frac{\partial^2 c}{\partial x^2} + \frac{K_h w_s\beta}{K_v}\frac{\partial H}{\partial x}\frac{\partial c}{\partial x} + \left[\frac{w_s^2}{K_v}\beta + \frac{K_h w_s}{K_v}\left(\beta\frac{\partial^2 H}{\partial x^2} + \frac{\partial \beta}{\partial x}\frac{\partial H}{\partial x}\right)\right]c = -\left|\frac{2uU}{\pi}\right|,$$

$$\frac{\partial H}{\partial \tau} = aK_h\frac{\partial^2 c}{\partial x^2} + \lambda\frac{\partial}{\partial x}\left[\beta\frac{\partial H}{\partial x}c\right],$$

where the sediment parameter β is defined by:

$$\beta = \frac{1}{1 - \exp\left(-\frac{w_s}{K_v}H\right)}$$

and r the bed friction coefficient. This parameter r is taken equal to sU with U the characteristic velocity. Using the derivation in Sect. 1.4.1, this can be

replaced by the conversion factor F_{conv} to give a more representable morphodynamical model.

When applying this conversion factor the results of this 1-dimensional model and the results of the 2DV-model should approximately be the same apart from the inclusion of along-channel diffusion in the 1D concentration equation.
When the conversion factor is not used the results will gradually differ as the sea bed evolves.

Chapter 3

Results

In this section the results of the 2DV morphodynamical model developed in the previous section are discussed. First, the hydro- and morphodynamic results of the developed model are shown for a characteristic domain and a characteristic set of parameters, given in Table [3.1]. In this first experiment, the bed is assumed to be flat and hence not in morphodynamical equilibrium. Next, the equilibrium of the sea bed is computed.

Furthermore, a sensitivity analysis concerning some of the important parameters is performed:

- the length of the inlet system L,
- the depth of the inlet system at the inlet I and II $H(0)$ and $H(L)$,
- the partial slip parameter s, defining the friction of the water with the seabed,
- the vertical eddy viscosity A_v that models the mixing of the water in the vertical direction,
- the settling velocity w_s of the suspended sediment in the water,
- the relative phase difference of semi-diurnal tide ϕ between inlet I and II.

The influence of these parameters is displayed on the water velocity and sediment concentration for flat sea beds, and on the equilibrium solutions.

Finally, the results of the 2DV-model are compared with a one-dimensional model. For this, four different types of one-dimensional models, introduced in section 3.3, are considered:

- A depth-averaged model with settling parameter β and the conversion factor F_{conv},

Table 3.1: Table describing all parameters in the basis system

Description	Symbol	Unit	Value
Partial slip friction parameter	s	ms^{-1}	0.014
Semi-diurnal angular tide frequency	σ	s^{-1}	$1.4 \cdot 10^{-4}$
Length of the inlet system	L	km	59
Depth of the inlet system at the entrance	H_0	m	11.7
Typical density of the water	ρ_0	kgm^{-3}	1020
Amplitude of the semi-diurnal tide	A_{M_2}	m	0.62
Phase difference of semi-diurnal tide	ϕ_{M_2}	degrees	54
Vertical eddy viscosity	A_v	m^2s^{-1}	0.012
Horizontal eddy viscosity	K_h	m^2s^{-1}	100
Settling velocity	w_s	ms^{-1}	0.01
Density of the sediment	ρ_s	kgm^{-3}	2650
Erosion coefficient	a	-	10^{-5}
Gravitational acceleration	g	ms^{-2}	9.81
Grain size of the sediment	d_s	m	$2 \cdot 10^{-4}$

- A depth-averaged model with settling parameter β,
- A depth-averaged model without settling parameter β,
- A depth-integrated model without settling parameter β.

The equilibrium solutions for different parameter choices are compared between the 2DV-model and these four 1D-models.

3.1 Morphodynamics on an idealized domain

The 2DV-morphodynamic model derived in chapter 2 computes the sea bed evolution on the long time scale in four steps: first, for a given bathymetry, the sea level ζ^0, the along-channel water velocity u^0, the sediment concentration c^{00} are calculated and finally the sea bed evolution z_b is obtained.

In this section the width of the inlet system is assumed to be constant and the depth of the inlet at both entrances are assumed to be equal as well. Furthermore, the amplitude and phase difference of tides between the two inlets is assumed to be constant in time.
The values of the parameters used in this section are shown in table 3.1 showing the values of parameters showed in this section.

3.1.1 Water motion

The complex amplitude of the sea level ζ^0 is obtained using equation (A.14). The actual along-channel sea level $\hat{\zeta^0}$ during a semi-diurnal tidal cycle is given by $\hat{\zeta}^0(t,x) = \mathbb{R}(\zeta^0(x)e^{i\sigma t})$. An example of the sea level for a flat sea bed during

Figure 3.1: Sea level during a tide cycle in base system

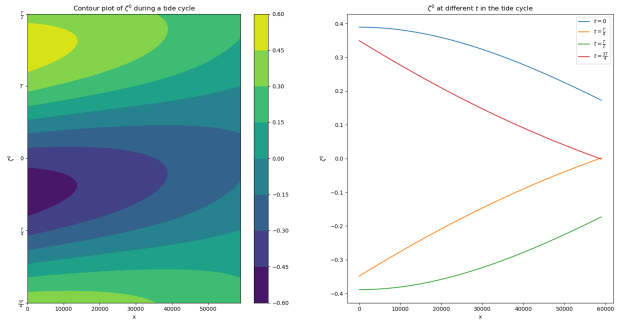

Figure 3.2: Amplitude and argument of sea level for default parameter values, see table 3.1

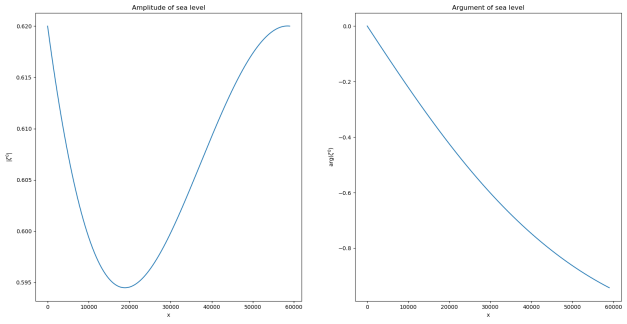

a semi-diurnal cycle can be seen in figure 3.1. It follows that during a tide cycle the sea level will change between A_{M_2} to $-A_{M_2}$ at both inlets because of the relative phase difference ϕ, this will happen at different time t.

Although the sea bed evolution is dependent on time, it is assumed constant over a tidal cycle, as the sea bed evolution is obtained after averaging over a tidal cycle, i.e. the bed evolves only on the longer morphodynamic time scale τ.
Instead of plotting a time series as in Figure [3.1], the free surface elevation can also be captured in terms of amplitude and relative phase difference. These are defined by:

$$\text{Amp}(\zeta^0) = |\zeta^0|,$$
$$\text{Phase}(\zeta^0) = \text{atan2}(\Im(\zeta^0), \Re(\zeta^0)).$$

In figure 3.2 the amplitude and phase of the free surface elevation. The amplitude of the sea level is greatest at both entrances of the inlet system and

Figure 3.3: Water velocity at $t = 0$ in base system

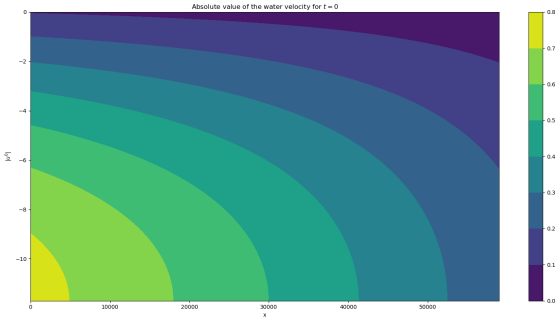

decreases slightly in the interior. Furthermore, the argument in the inlet system increases linear from 0 to ϕ. Using the free surface elevation, the water velocity in the along-channel direction u^0 can be obtained. The expression for u^0 is:

$$u^0(x,z,t) = \Re\left[-\frac{g}{i\sigma}\frac{\partial \zeta^0}{\partial x}\left(1 - \frac{s\cosh(\beta z)}{A_v\beta\sinh(\beta H) + s\cosh(\beta H)}\right)e^{i\sigma t}\right]$$

Thus, in the x-direction the water velocity has a one-on-one relation with the derivative of the sea level, while the water velocity in the z-direction only depends on the term $\cosh(\beta z)$ and depends parametrically on water depth.

In Figure [3.3] the water velocity at $t = 0$ is plotted as a function of depth on the vertical axis and the distance from the first inlet on the horizontal axis. In the z-direction u^0 is decreasing as it get closer to the sea bed at $z = -H$ which is evident from the the expression for u^0. Indeed, for $s/to/infty$, the boundary condition becomes $u = 0$ at the bed $z = -H$. For the x-direction the velocity is monotonically decreasing, which is related to the decrease of the derivative of ζ^0 in the positive x-direction.

3.1.2 Sediment concentration

To obtain the suspended sediment concentration, necessary to calculate the bed evolution, only the residual component of the absolute value of the water velocity at the sea bed is needed. For this, the first Fourier coefficient denoted by a_0, is calculated, resulting in:

$$a_0 = \frac{2}{T}\int_0^T |u^0(x,z,t)|\mathrm{d}t = \frac{2g}{\sigma\pi}\left|\frac{\partial \zeta^0}{\partial x}\left(1 - \frac{s\cosh(\beta H)}{A_v\beta\sinh(\beta H) + s\cosh(\beta H)}\right)\right|$$

This term only depends on x and is similar to the absolute value of u^0 in Figure

Figure 3.4: Amplitude and argument of the water velocity in base system

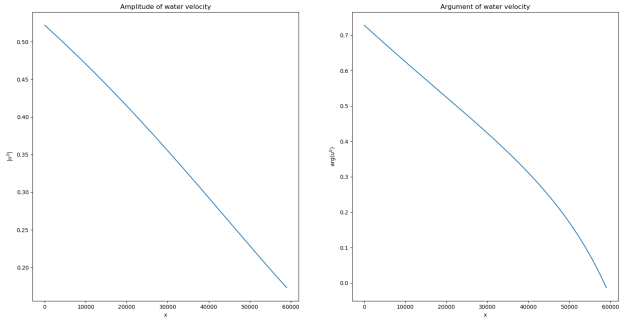

Figure 3.5: Sediment concentration at $t = 0$ in base system

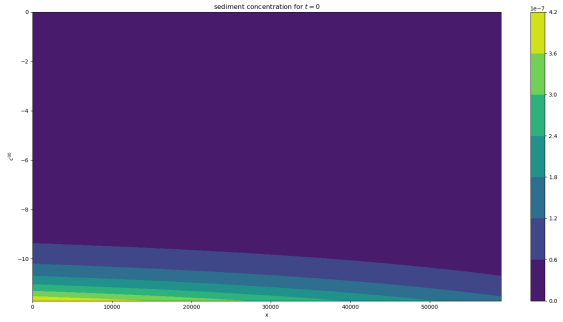

[3.4] for a flat sea bed and is monotonically decreasing.

As discussed in section (2.2.2, the sediment concentration in a double inlet system can be computed with the main balance $w_s \frac{\partial c^{00}}{\partial z} + K_v \frac{\partial^2 c^{00}}{\partial z^2} = 0$, ignoring diffusion of sediment in the x-direction results in the expression:

$$c^{00} = \frac{\rho_s s a a_0}{g' d_s} \exp\left(-\frac{w_s}{K_v}(H+z)\right).$$

In figure 3.5 the sediment concentration for $t = 0$ with the characteristic parameters is displayed for a flat sea bed. Most of the sediment will be concentrated around the sea bed and in the longitudinal direction there is some variation in the sediment concentration too.

3.1.3 Sea bed evolution

As a final step the sea bed evolution is computed using the non-homogeneous diffusion equation, with the sea bed prescribed at the inlets. The resulting

ref to equation

Figure 3.6: Sea bed evolution after one semi-diurnal tide cycle in base system

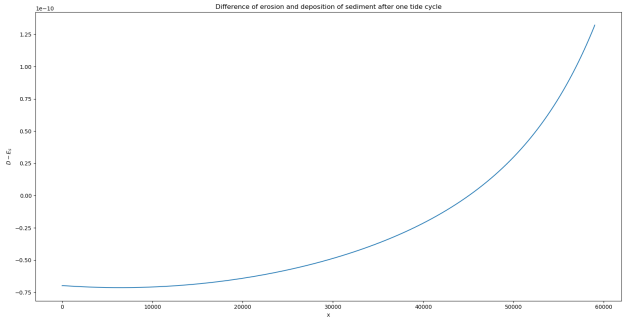

change in sea bed after one semi-diurnal cycle is displayed in figure 3.6. The change in sea bed is mainly determined by the second derivative of c^{00}. Since this term is very small, only after a large number of tidal cycles there will be significant change in the location of the sea bed. From the figure it follows that the sea bed will be slightly deepened in the entire inlet system.

3.1.4 Equilibrium solutions

Using the tidally averaged concentration the equilibrium sea bed can now be calculated. This can be done by iteratively updating the sea bed H: the initial bathymetry is used to get the water motion and suspended sediment concentration, after which the sea bed is updated; with the updated sea bed the new water motion and suspended sediment concentration are calculated resulting in a sea bed update. This loop is repeated until an equilibrium is reached.
Figure 3.7 shows the equilibrium solution in a system with the characteristic parameters.

Finding an equilibrium using the above approach is typically a very slow process because the changes in the sea bed become smaller when approaching the equilibrium. When the sea bed is in equilibrium the changes in the sea bed are equal to zero, thus minimizing the sea bed evolution term $D - E_s$ for different H is a way to approach the equilibrium solution and is much faster. This minimizing sea bed is closer to the equilibrium solution than a flat sea bed. Because of this, the iterative process described above will converge in less tidal cycles to the equilibrium when taking the minimizing sea bed H_{min} as the initial sea bed.

The basis functions over which the minimizing equilibrium solution is to be found is the collection of sinus modes

$$H(x) = \sum_{i=1}^{\infty} d_i \sin\left(\frac{i\pi x}{L}\right).$$

Figure 3.7: Equilibrium solution for the characteristic parameters

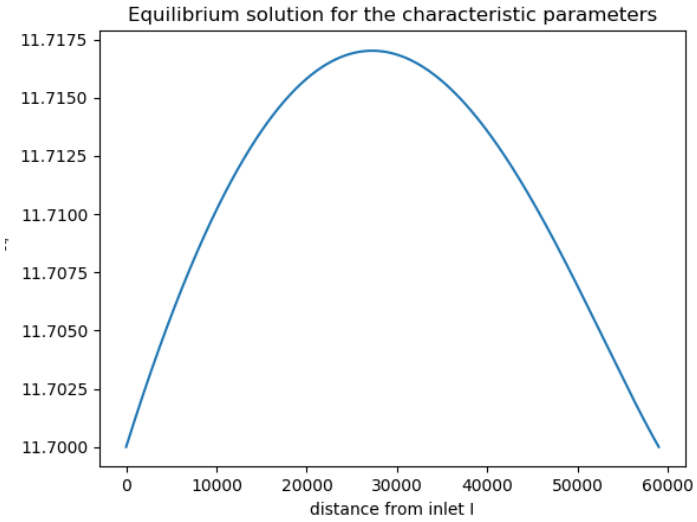

By truncating the infinite series, taking n terms into account, this will result in an approximation of the morphodynamic equilibrium sea bed. Increasing n will lead to a better approximation, as shown in figure 3.8. In this figure, it is shown that by increasing the number of modes i the difference of the resulting minimizing sea bed H_i with the actual equilibrium $|H_{eq} - H_i|$ decreases. Thus more modes result in higher accuracy.

3.2 Parameter sensitivity

In the previous section the equilibrium for one specific set of parameters was obtained. In this section the sensitivity to parameters of the resulting equilibrium solution is investigated. The parameters we focus on are:

- Friction parameter s; this term appears in the expressions for c^{00} and u^0 as well as in the differential equation for ζ^0,
- the settling velocity of the suspended sediment w_s. This parameter appears in the expression for c^{00} and strongly determines its vertical profile,
- the vertical eddy viscosity and diffusivity coefficients A_v and K_v,
- the relative phase difference ϕ, as this parameter has influences on the water motion in the inlet system,
- the length of the inlet system and the depth at the seaward sides. These parameters describing the domain as the boundary conditions are greatly influenced by them. Therefore studying the influence of them is important.

Figure 3.8: L_2-norm of difference of minimizing sea bed with equilibrium for different number of modes

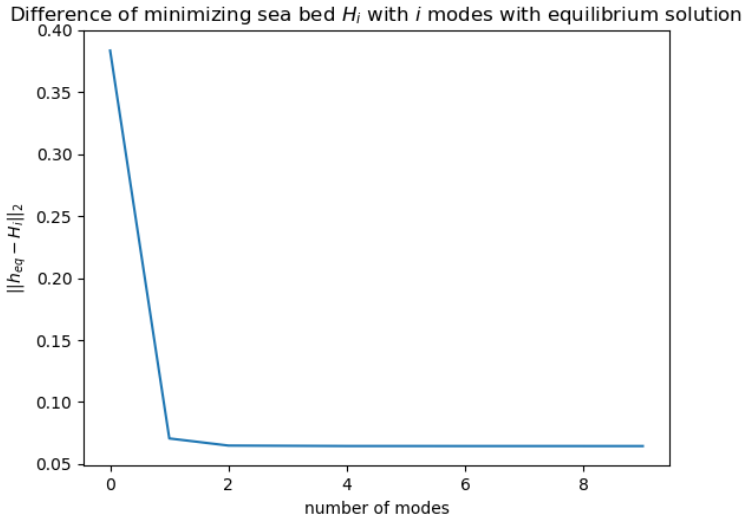

The value of each of these parameter will be varied in an interval and its influence on the resulting equilibrium solution will be quantified.
Equilibrium solutions are obtained with time integration with a global minimizing sea bed of one mode as initial condition. If the existence of multiple equilibrium solutions is investigated local minimizing sea beds can be used to find more than one equilibrium solutions for the same set of parameters.

3.2.1 Friction with the sea bed

The bed friction has a large influence on the water velocity in the water column and at the sea bed. This strongly influences the magnitude of the suspended sediment.

In figure 3.9 the equilibrium solutions for different values of s are shown. Tt follows that the maximum depth of the equilibrium sea bed increases as s is increased. Furthermore, the shape of the equilibrium solution seems to get more symmetrical around $x = \frac{L}{2}$ as s is increased. This observation is continued in Figure 3.10, where a contour plot of equilibrium bed profiles is plotted as a function of the distance from the first inlet (horizontal axis) and for different values of s (vertical axis). The relation between the maximum depth of the equilibrium sea bed and the friction is shown in Figure 3.11 and appears to be approximately linear with $\max(z_b)$ increasing as s is increased.

Figure 3.9: Equilibrium solution with different values for s

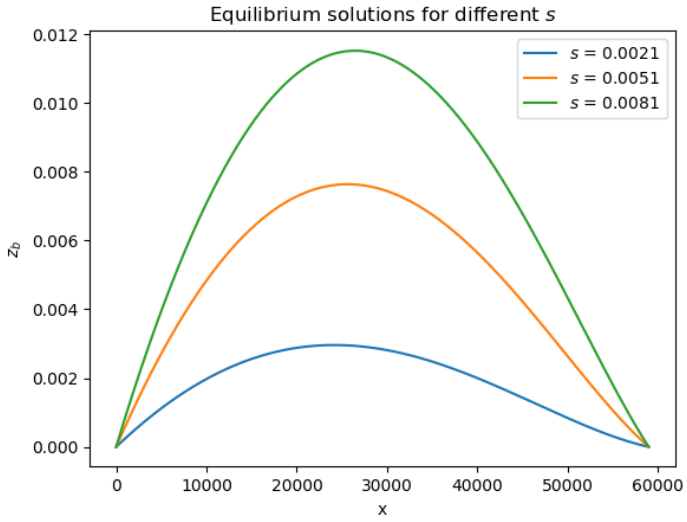

Figure 3.10: Contour plot of equilibrium solutions with different values for s

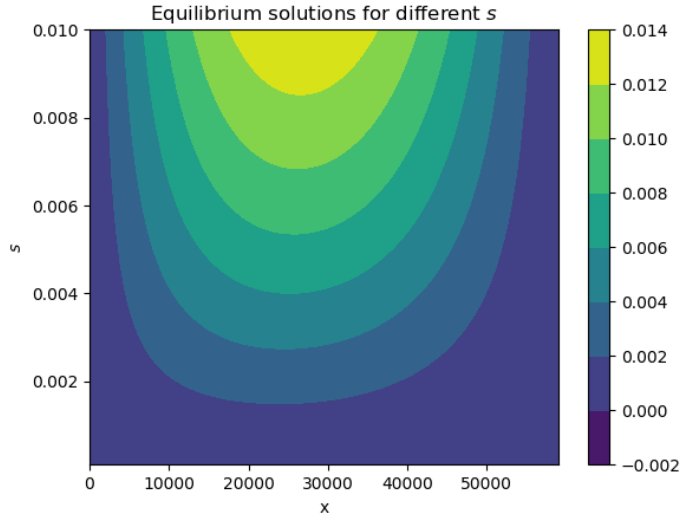

Figure 3.11: xtremes of equilibrium solution with different values for s

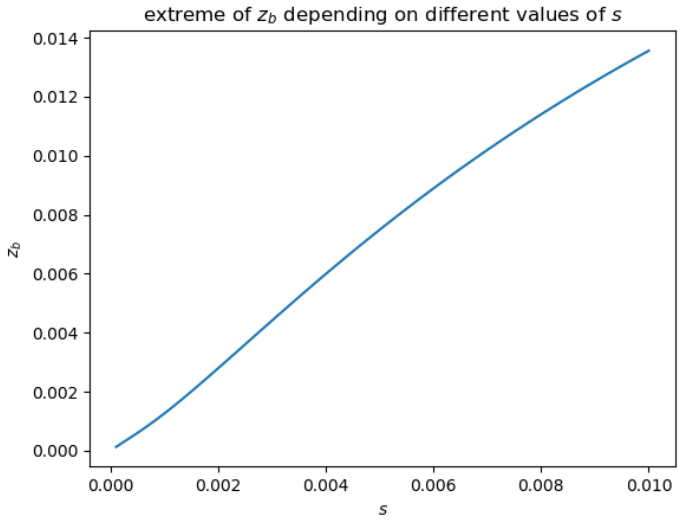

3.2.2 Settling velocity

Next, the sensitivity of the morphodynamical equilibria with respect to the settling velocity w_s is investigated. As w_s increases, the deposition of sediment also increases. Hence it is expected that the resulting equilibrium sea bed is be more shallow as w_s is increased.

In figure 3.12 three equilibrium bed profiles are shown for three different values of w_s and confirms this correlation. A contour plot of equilibrium bed profiles as a function of values for w_s and the distance to inlet I can be seen in Figure (3.13). Furthermore, Figure (3.14) displays the maximum of the equilibrium sea bed as a function of values for w_s and shows a monotone relation between w_s and $\max(z_b)$ where $\max(z_b)$ decreases as w_s increases.

Figure 3.12: Equilibrium solution with different values for w_s

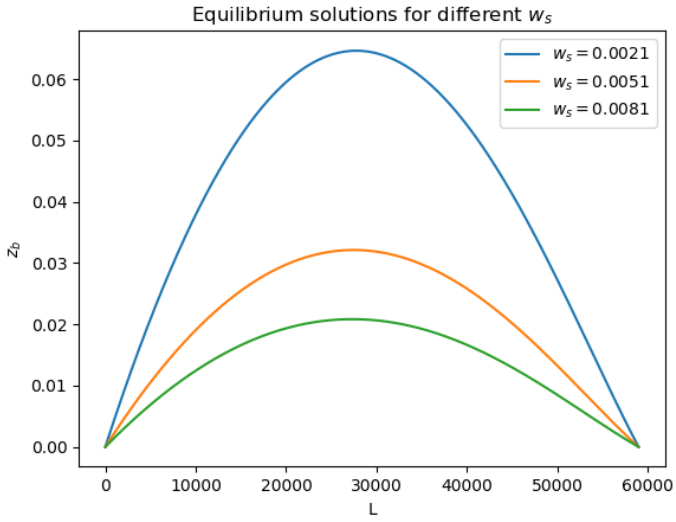

Figure 3.13: Contour plot of equilibrium solutions with different values for w_s

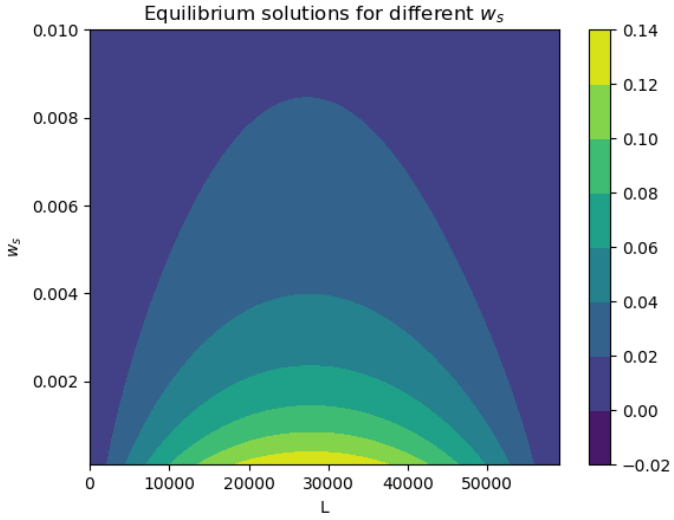

Figure 3.14: Extrmes of equilibrium solutions with different values for w_s

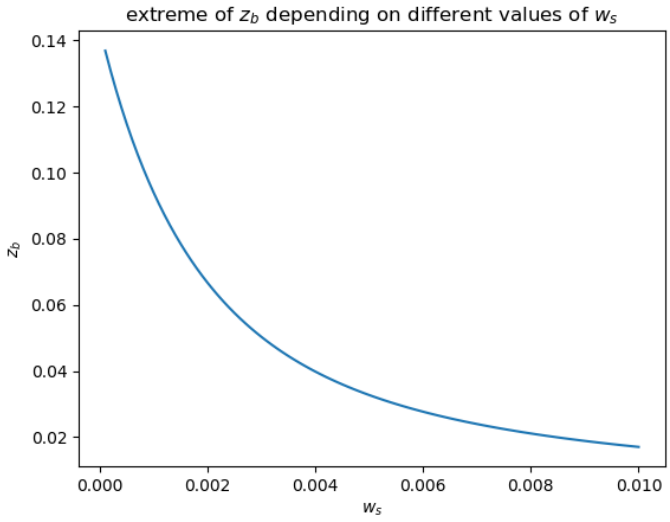

3.2.3 Vertical eddy viscosity and diffusivity coefficient

Hypothesising what the contribution of the vertical eddy viscosity and diffusivity to the equilibrium sea bed is difficult as both the deposition of sediment and erosion is not explicitly dependant on A_v or K_v. But from the expression for c^{00} it shows that the second derivative decreases as K_v is increased which suggests that the equilibrium sea bed gets shallower as K_v is increased.
This can be caused by the fact that more vertical mixing of water results in the suspended sediment being more uniformly distributed in the domain and less suspended sediment being near the sea bed, with less sediment in the region of the sea bed less will be deposited.

The equilibrium bed profiles shown in figure (3.15) are quite different for different values of the vertical mixing. Instead, the value of first mode of the minimizing sea bed as a function of different values for w_s, see Figure (3.16), give a clearer image of the relation. Near the parameter value of $A_v = 0.03$ there is a sudden change in minimizing sea bed which suggests the existence of multiple branches of equilibrium solutions.

Thus, instead of calculating equilibrium solutions with globally minimizing sea beds, locally minimizing sea bed can be used to find multiple equilibrium sea bed with the same parameter values. In figure (3.17) the extremes of these equilibrium solutions obtained from locally minimizing sea beds are shown as a function of different values of A_v.
This figure clearly shows two separate branches of equilibrium solutions: one type of equilibrium solution has an extreme larger than the water depth at the

Figure 3.15: Equilibrium solution with different values for A_v

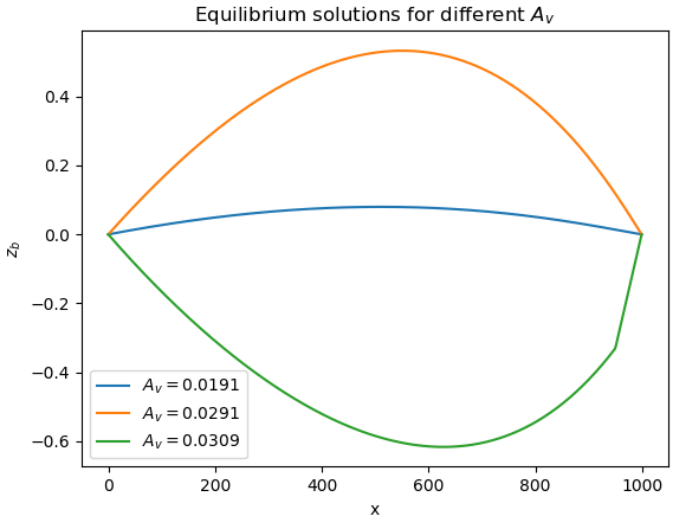

Figure 3.16: Minimizing d_1 with different values for A_v

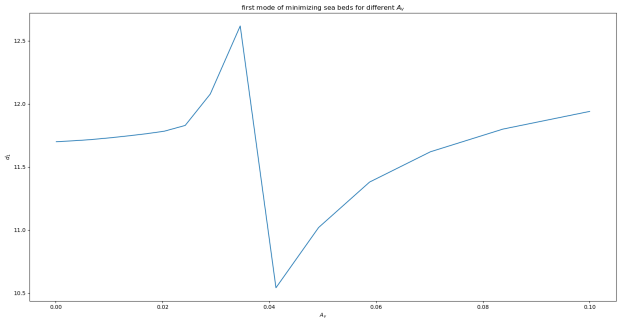

Figure 3.17: Extremes of equilibrium solutions for different values of A_v

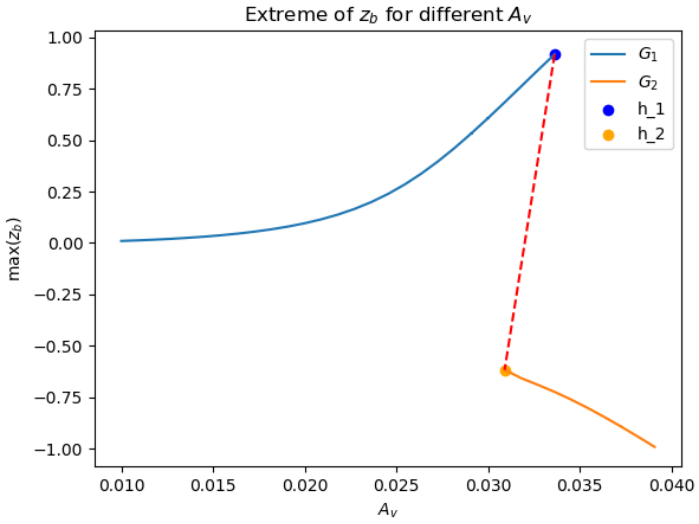

seaward sides and one with an extreme smaller than the water depth at the seaward sides.
When using an equilibrium solution for a specific value of A_v as the initial condition and varying the value for A_v slightly the subsequent new equilibrium solution will generally be on the same branch as the initial condition. But for two limit points this is not the case: These limit points are denoted in figure (3.17) as h_1 and h_2. When increasing A_v from h_1 as an initial condition no equilibrium solutions can be found and the time integration will always diverge from the initial condition.
For the second limit point h_2, when A_v is decreased and h_2 is taken as initial condition the resulting equilibrium solution will have an extreme which is larger than the water depth at the seaward sides thus lies on the other branch.

The existence of these two limit points suggests a third unstable branch connects the two limit points. Because this branch will be unstable finding solutions on this branch are impossible, but using minimization to find approximations might be possible. Finally figure (3.18) shows the two equilibrium solutions for $A_v = 0.0336$. This figure shows the difference in shape of the equilibrium solution.

Figure 3.18: Two equilibrium solution for $A_v = 0.0336$

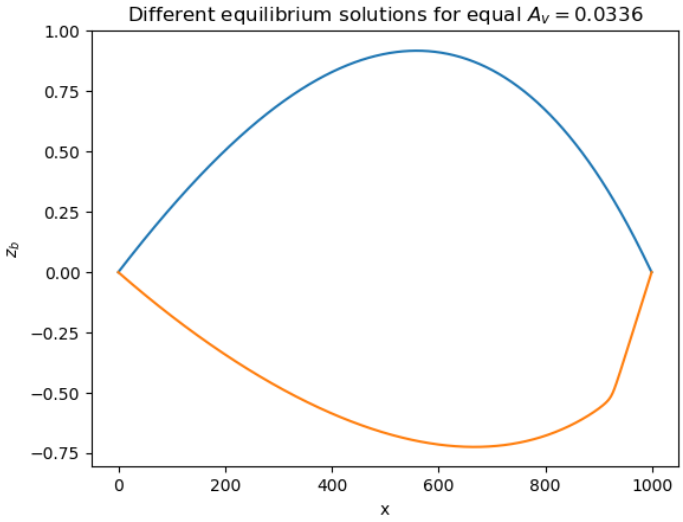

3.2.4 Relative phase difference

From the set of parameters the relative phase difference ϕ is one of the most impactful parameters on the resulting equilibrium solution to the sea bed evolution equation. For large difference in phase the water velocity will be more uniform along the inlet system, this is because during the semi-diurnal the water velocity will generally only travel in one direction. Because of this uniformity the second derivative of c^{00} will be small.

For small ϕ the water can travel from both inlets towards the centre of the inlet system at the same time which causes a lot of sediment to accumulate in the middle. For $\phi \to 0$ the shape of equilibrium solutions will not have the characteristic sinusoid shape. The equilibrium sea bed profile for $\phi = 1°$ can be seen in Figure 3.19. Important to note that instead of the interior being deeper in the middle with the characteristic parameters this profile is shallower in the interior. This is caused by the fact that the small phase difference results in approximately equal waves coming from the inlets to the centre resulting in a large inference near the centre of the inlet system.

From the assumption that the water velocity will be more uniform as ϕ increases a relation can be obtained; for larger ϕ the sea bed will be more flat. Figure (3.20) shows the equilibrium solution for three different values of ϕ. The profile of the sea bed for $\phi = 21$ draws the attention as the shape is not sinusoid and the sea bed is more shallow in the interior compared to the inlets instead of deeper. From this there seems to be a value for which the type of profile switches from being deeper in the interior to being shallower.

Figure 3.19: Equilibrium solution with different values for ϕ

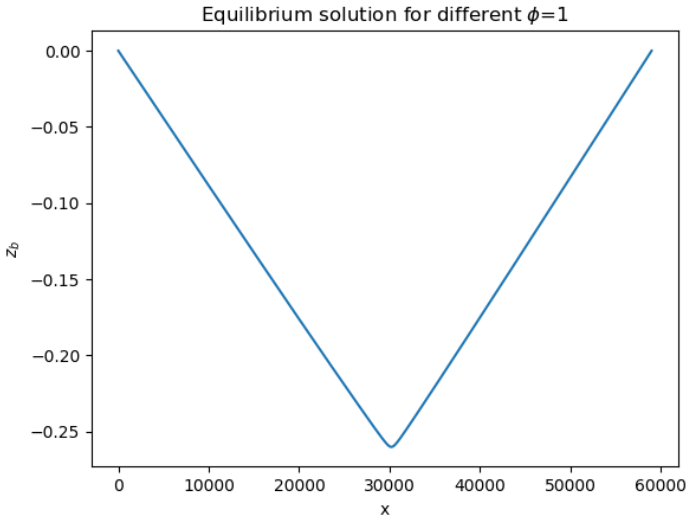

Figure 3.20: Equilibrium solution with different values for ϕ

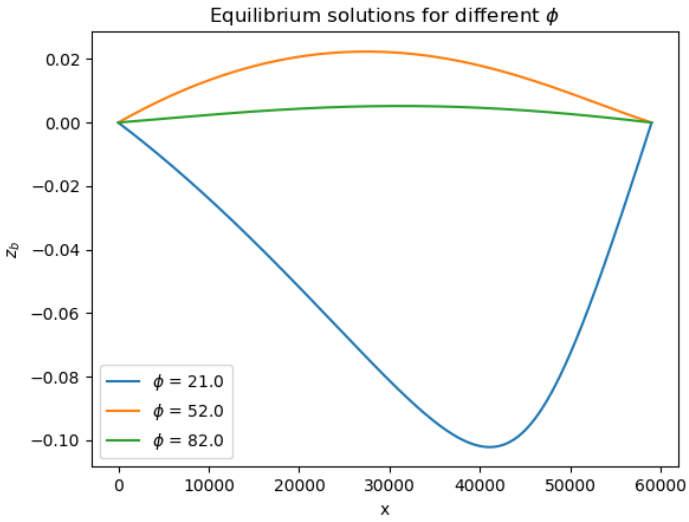

Figure 3.21: Extremes of equilibrium solutions for different values of ϕ

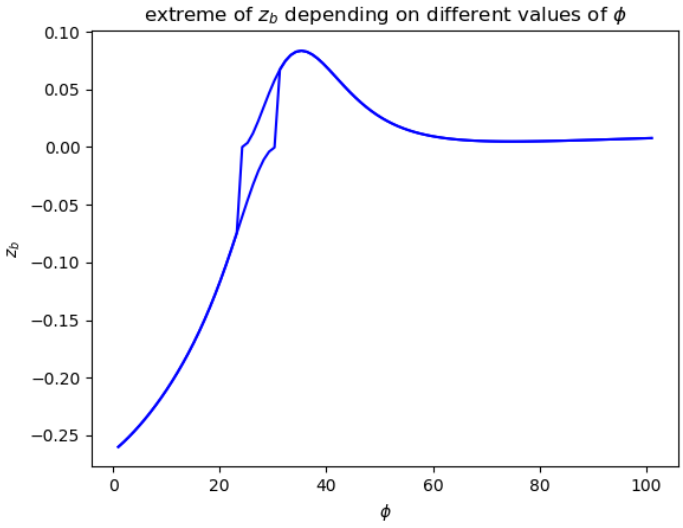

Figure 3.22: Equilibrium solution for $phi = 1$

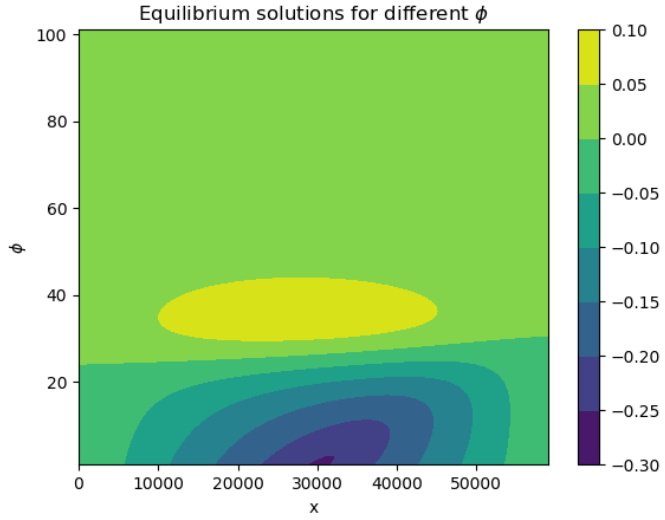

To give insight in this change the extremes of all equilibrium bed profiles from $\phi \in [0, 100]$ are plotted in Figure(3.21). From this figure it seems that for $\phi \in [20, 35]$ there is an intermediate stage where the profile of the equilibrium solution has two extremes: one minimum and one maximum. Figure (3.22) shows an contour plot of the equilibrium solutions for different values of ϕ.

Figure 3.23: Equilibrium solution with different values for L

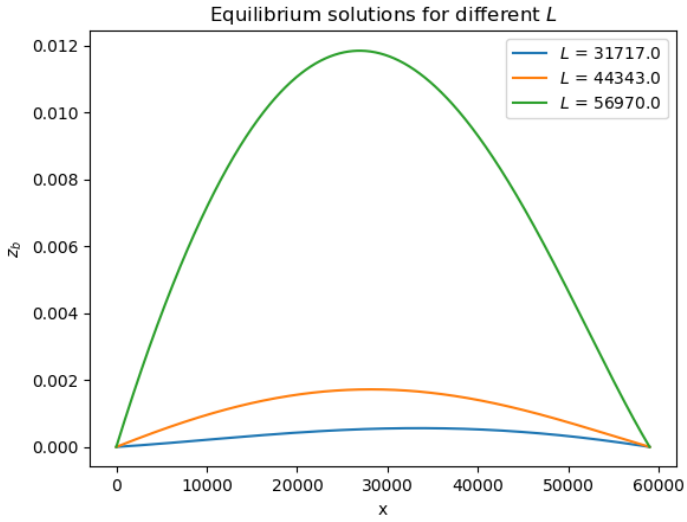

3.2.5 Length of inlet system

The length of the inlet system influences the Reynold's number thus can influence balances between the individual terms in the water velocity equation. Longer inlet systems have larger Reynolds number thus the fluid flow will be more turbulent and will result in more mixing of water. Furthermore, advective flow will be more important. But both diffusive and advective flow are not present in this 2DV-model.

First, Figure (3.23) shows three equilibrium solutions for three different values of L and Figure (3.24) shows the equilibrium solutions as a function of the length of the inlet system L and the distance from inlet I in an contour plot. it comes apparent that longer systems lead to deeper sea beds, this is probably caused by the increase of mixing caused by the increase of turbulent flow. Finally, Figure (3.25) shows the extremes of the equilibrium solutions as a function of L. This figure the relation between the maximum depth of the equilibrium sea bed and the length of the inlet system is monotone.

Figure 3.24: Minimizing d_1 with different values for L

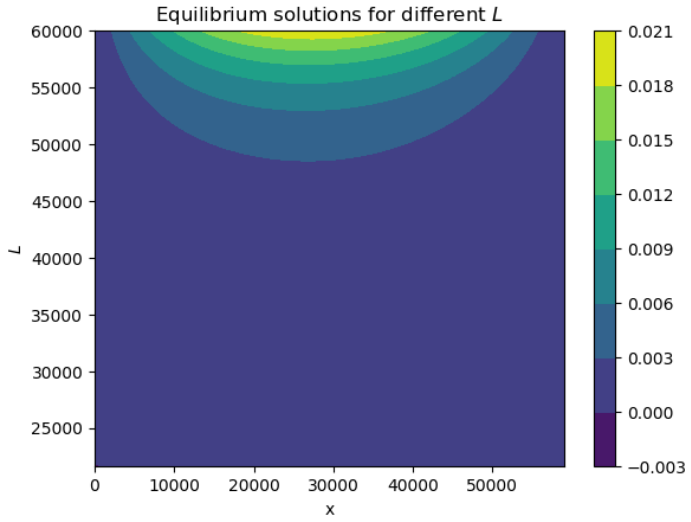

Figure 3.25: Minimizing d_1 with different values for L

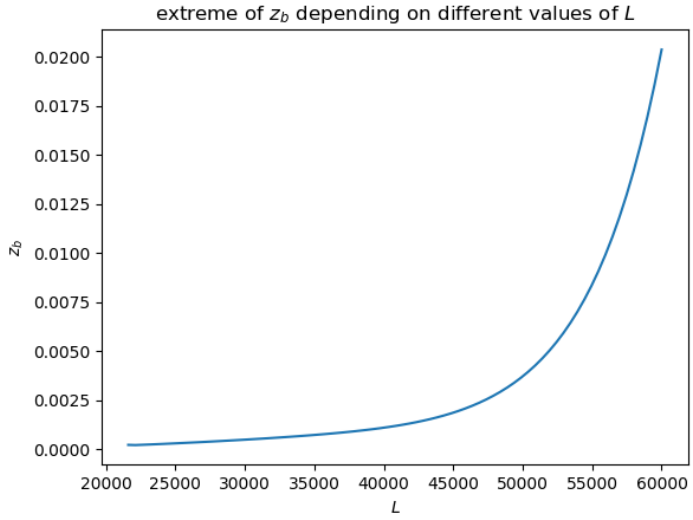

Figure 3.26: Equilibrium solution with different values for h_0

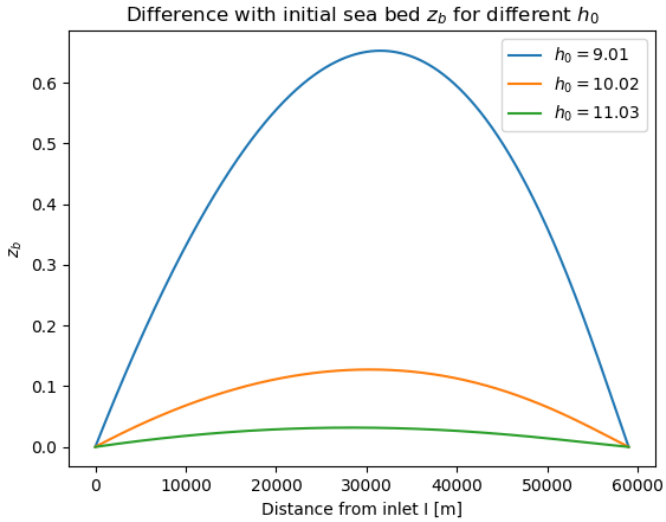

3.2.6 Depth of inlet system

The last sensitivity analysis will be on the depth of the entrances of the inlet system. Figure 3.26 shows three equilibrium solutions for three different values of the water depth H and Figure 3.27 displays the extremes of the equilibrium solutions as a function of the water depth H. From these figures it seems that in general when the water depth gets smaller the sea bed gets deeper compared to the water depth at the seaward sides. But at around $H = 8.6$ the extreme of the equilibrium solution changes drastically.

This drastic change in extreme value of equilibrium solution could suggest the exitence multiple equilibrium solutions for equal h_0. Further investigation can be done by analysing a contour plot of equilibrium sea beds as a function of H close to this tipping point. Figure (3.29) shows all equilibrium solutions for this range and the cause for the inflections points in minimizing d_1 is the sudden change of profile. The cause for the sudden change in extreme value is a fast change in the shape of the sea bed. But from this investigation it is clear that two equilibrium for the same value does not exist. The critical value that signalizes the change in equilibrium profile divides the equilibrium sea beds in two families. One family of equilibrium solutions has an interior entirely deeper than the water depth at the sea beds and a second family with its interior shallower than the water depth at the seaward sides.

Figure 3.27: Extremes of equilibrium sea beds for as a function of water depth at inlet

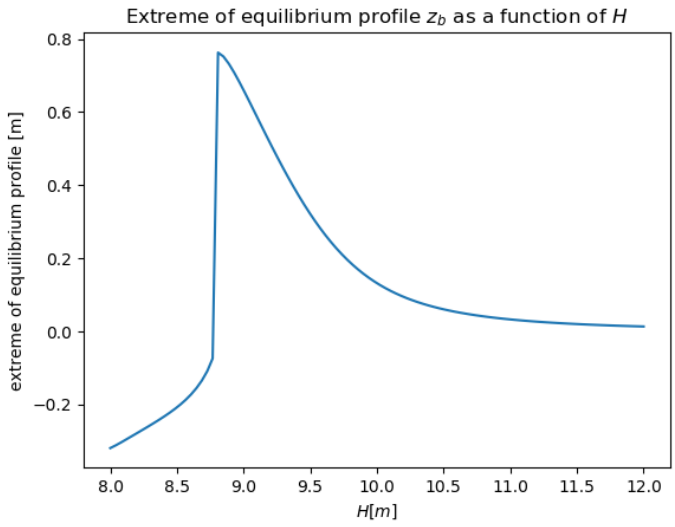

Figure 3.28: Contour plot of equilibrium solutions as a function of water depth and distance from inlet

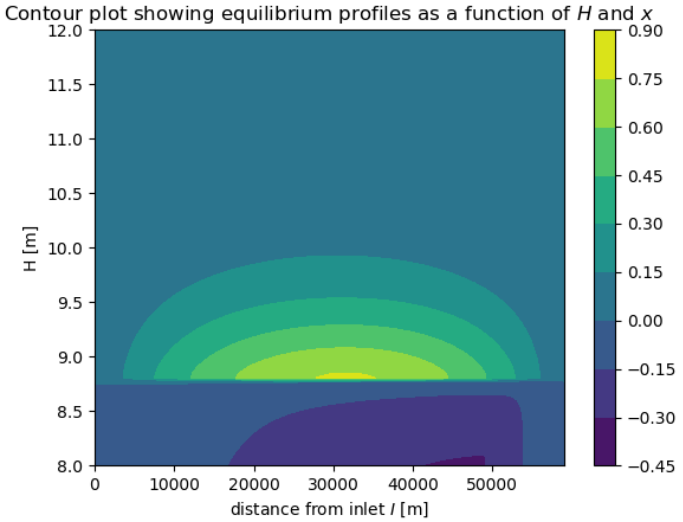

Figure 3.29: Zoomed in contour plot of equilibrium solutions as a function of water depth and distance from inlet

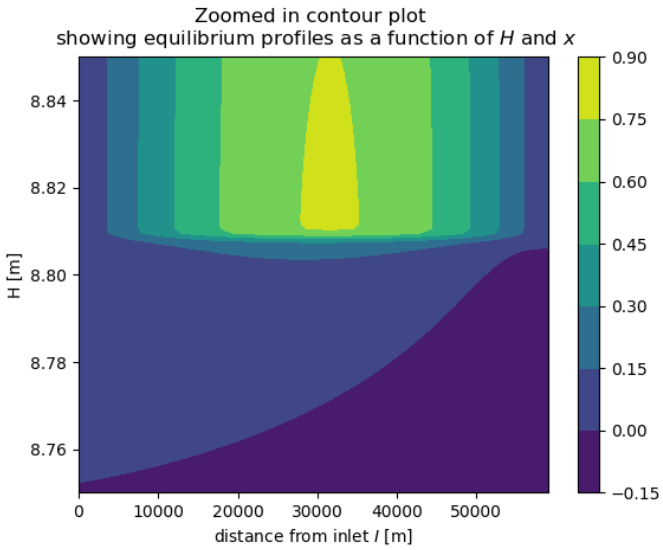

3.3 Comparison with depth-averaged models

In the study of morphodynamics, usually depth-integrated models have been used. In these types of models there is no dependency on the z-direction thus the water velocity at the sea bed is not calculated explicitly. This velocity at the sea bed is very important in both the sediment concentration and the sea bed evolution term.

In depth-averaged models this velocity at the sea bed is related to the depth-averaged velocity since the vertical structure of the velocity is unknown. The influence of this approximation is important to investigate. Also, to capture the vertical structure of the suspended sediment concentration in a depth-averaged model, a deposition parameter β that depends on the water depth is introduced.
To get a better estimate of the velocity at the sea bed, the depth-averaged velocity is multiplied by a conversion factor F_{conv}. It is expected that the morphodynamic behaviour will be similar with the 2DV model.

3.3.1 Water motion

As expected, the addition of the conversion factor F_{conv} causes both the free surface elevation ζ^0 and the water velocity u^0 to be the same in the 1-D and the 2-D model. This can be seen in Figs. 3.30 and 3.31, which show the free surface elevation and water velocity for a spatially uniform sea bed $H = h_0$. The free

Figure 3.30: Difference in free surface elevation with uniform sea bed in 1D and 2D models

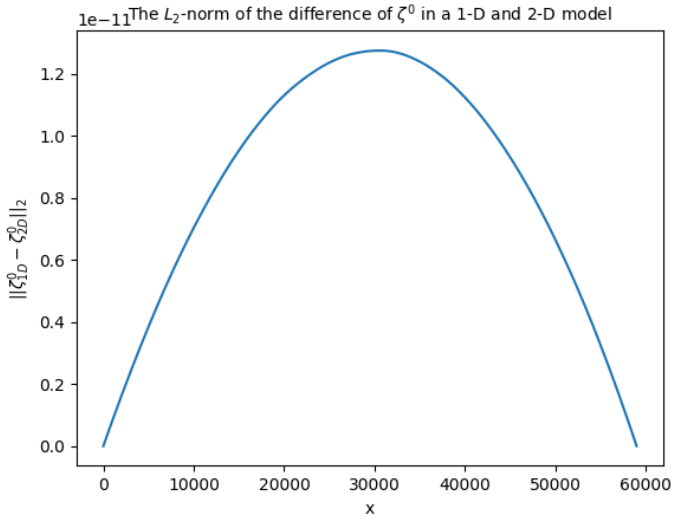

Figure 3.31: Difference in water velocity with constant sea bed in 1D and 2D models

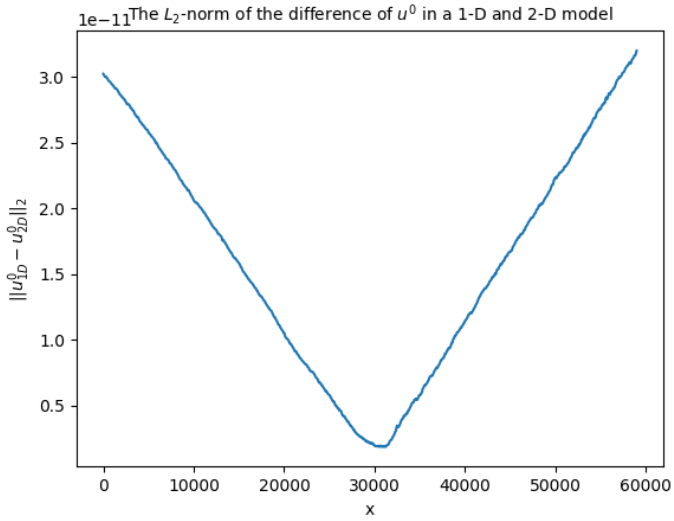

Figure 3.32: Free surface elevation with non-constant seabeds in 1D and 2D models

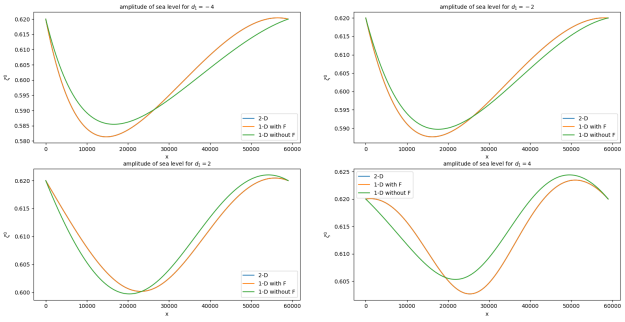

Figure 3.33: Water velocity with non-constant seabeds in 1D and 2D models

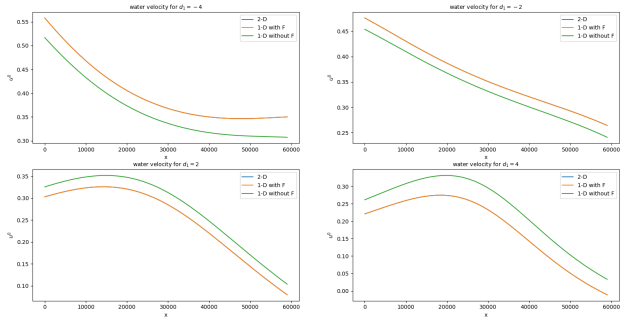

surface elevation and water velocity at the bottom for the 2-dimensional model are compared to the free surface elevation and the depth-averaged velocity in the 1-dimensional model.
The small difference between the result of both models can be accounted for by the truncation error in the numerical scheme but should not affect the equilibrium solutions.

When the conversion factor is not used to compute the sea level and the water velocity the solutions of the 1-D and 2-D model will diverge from one another. Figures (3.32) and (3.33) show respectively the free surface elevation and water velocity for sea bed $H = h_0 - d_1 \sin\left(\frac{\pi x}{L}\right)$ where d_1 is varied in all subplots. The difference in both the free water surface and water velocity when F_{conv} is not used is apparent and can lead to quite different morphodynamic equilibrium solutions.

Figure 3.34: Difference in sediment concentration with constant seabed in 1D and 2D models

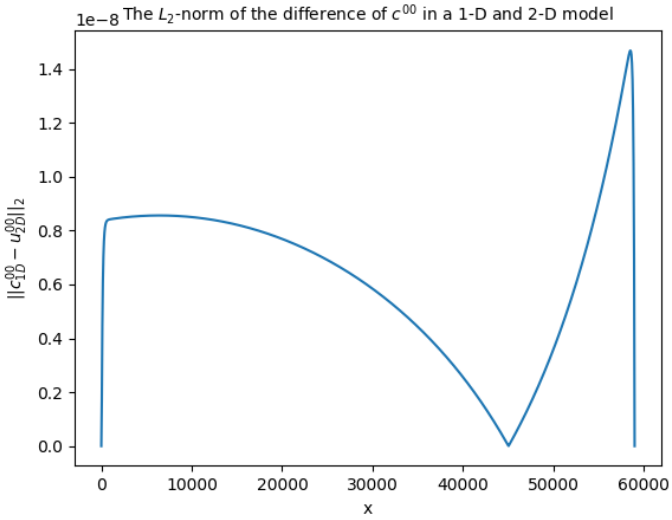

3.3.2 Sediment concentration

When calculating the suspended sediment concentration in a depth-averaged model, the conversion factor F_{conv} can be used to obtain the water velocity at the sea bed H. However, when using F_{conv} in the bottom boundary condition does not result in equivalent suspended sediment equations in the one-dimensional and two-dimensional model as the one-dimensional model includes a diffusion term in the horizontal direction which is not present in the two-dimensional model.
From Fig. 3.34 it is shown that this addition does not greatly influence the sediment concentration as the difference between the sediment concentration from the one-dimensional model and the depth-averaged sediment concentration from the two-dimensional model is marginal.

However, when F_{conv} is not used the sediment concentration computed in a one-dimensional can differ from the two-dimensional model. Figure 3.35 shows the sediment concentrations in both types of model with and without F_{conv} used. Because, for the same water depth H, the calculated sediment concentration in the one-dimensional model without using F_{conv} differs from the one-dimensional model with F_{conv} this means the two types of models will lead to different equilibrium solutions.

Figure 3.35: Sediment concentration with non-constant seabeds in 1D and 2D models

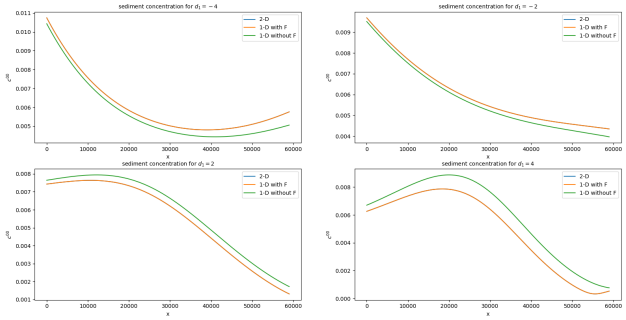

3.3.3 Equilibrium solutions

Because of the fact that both the water motion and sediment concentration yield exactly the same solutions it suggests that the sediment concentration will be equal as well. But because the equations describing the sea bed evolution differ in the one and two-dimensional models this is not the case. The one-dimensional model has an extra term added for the longitudinal diffusion.
This extra term in the one-dimensional model is not a large term but does lead to differences in equilibrium solutions. This can be seen in figure (3.3), where the equilibrium solutions from both models are compared. The equilibrium solution in the one-dimensional in less deep over the whole domain than the equilibrium solution in the two-dimensional model. Furthermore, the profiles differ in shape as well. The equilibrium solution in the one-dimensional model is less symmetrical as it has a inflection point near inlet II which the two-dimensional solution does not have. This inflection point can be caused by the longitudinal diffusion term.

But generally, the two solutions are close together and if the diffusion term is omitted this will lead to exactly the same sea bed.

Figure 3.36: Equilibrium solution in 1D and 2D models

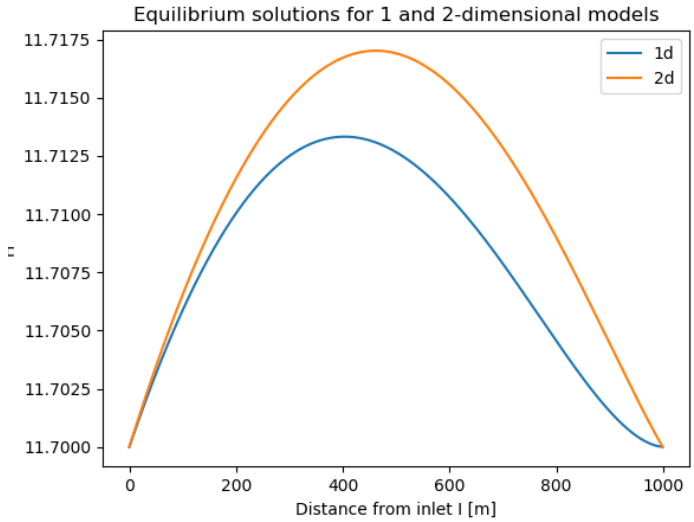

Chapter 4

Conclusion and discussion

4.1 Conclusion

This section discusses the conclusions that can be drawn from the research conducted throughout this article with respect to the research questions posed in section 1.2 and from new insights found.

4.1.1 Two-dimensional model for morphodynamics

It can be concluded that it is possible to construct a two-dimensional model without the structure in the vertical direction being averaged out. Furthermore, it is possible to numerically find solutions to the equations arising from this model and the computations are not too expensive.

From the model and numerical schemes equilibrium sea beds can be found for which the sea bed does not change any more. The model allows to investigate the influence of varying the values of single parameters to the resulting equilibrium solutions.

Following this parameter sensitivity study some anomalies were found. First of all, for some range of values of the vertical eddy viscosity and diffusivity A_v and K_v it is possible to have two separate equilibrium solutions. Although this range does not represent natural values for these particular parameters it can mean that for more sets of parameter values multiple equilibrium solutions exist.
Secondly, when increasing the water depth at the seaward sides H the profile of the equilibrium sea bed solution changes rapidly from an interior water depth deeper than the H to an interior water depth shallower than H. This phenomenon is interesting as the water depth at the seaward side does change quite frequently in practice.

In general, when varying a single parameter the existence of two types of equi-

librium sea beds, one shallower in the interior and one deeper, comes up a lot. For the range of parameter values this existence was shown for A_v, ϕ and H. And in between these types of equilibrium solutions an intermediate stage where the equilibrium sea bed has two extremes can exist.

In conclusion, it is possible to construct simplified models simulating the morphodynamics in double inlet systems and investigate the complexities. But in practice this type of model can not be used as it is simplified too much and a lot of factors have been removed in order to get solutions to the model.
As a proof of concept, this model shows potential and can expanded upon to include more processes and reflect the real-life situation more accurately.

4.1.2 Comparison with one-dimensional models

In addition to constructing a two-dimensional model for morphodynamics the results of the two-dimensional model were compared to the results of an already existing one-dimensional model. The most important difference between the two types of models is the structure in the vertical direction. To compute the erosion and deposition of suspended sediment in the system it is necessary to know the water velocity at the sea bed. One-dimensional models uses a characteristic water velocity to relate the depth-averaged water velocity to the water velocity at the sea bed. This value does not change when the sea bed is updated thus will not be a good representation of this relation.

This becomes clear when comparing the calculated water velocity for different sea beds. As the sea bed becomes less flat the calculated results diverge more from one another. This of course also results in different equilibrium sea beds.
From investigating this relation it became apparent that it is quite easy to relate velocity at the sea bed to the depth-averaged water velocity with a conversion factor F_{conv}. With this factor both the water velocity and the suspended sediment concentration will be exactly equal. The equilibrium solutions still differ as the one-dimensional differential equation for sea bed evolution includes diffusion in the longitudinal direction.

From this it is clear that is suffices to use one-dimensional models with conversion factor as it does not make the solutions more accurate but are easier to solve.

4.2 Discussion

Following the conclusion this section describes what, during the research, could have been done better or needs more investigating. Furthermore, recommendations on subsequent researches on this topic will be given.

First of all, although this type of two-dimensional model works well on double inlet systems, this type of model can not be used on single inlet systems in this form. This is because of the fact that the natural sea bed evolution in single inlets causes sediment to accumulate at the end of the inlet system. This will make the water depth at the end of the inlet equal to the free surface elevation at that point, which means that both finite difference and finite elements methods can not be used to solve any differential equations on that domain.

The numerical scheme used for the time integration can be investigated upon more. It is preferred to use a implicit scheme to ensure numerical stability, but the difference in erosion and deposition can never be implicit. Because of this, it is not known for what time steps the numerical scheme is stable. If this is known the numerical scheme can be optimized to compute equilibrium solutions faster by always using the largest time step for which the numerical scheme is stable.

The value of the diffusion parameter λ in the time integration has been chosen by previous research. But the sensitivity of this parameter has not been investigated. Varying this parameter can result in very different equilibrium solutions. The problem with choosing a smaller value is that the time steps which can be used have to be smaller too. Because of this, the computation times will increase significantly.

Furthermore, it is thesis it is chosen to only retain the leading order terms in the governing equations. The consequence of this is that both diffusive and advective flow is not present in the model. These types of flow can be very influential in a morphodynamical model. Thus, including these types of flow in the model can result in different equilibrium solutions and in more insights in the complexities of morphodynamics in double inlet systems.

Appendices

Appendix A

Appendix A

A.1 Width-averaged model

A.1.1 Width-averaged shallow water equations

Derivation of width-averaged shallow water equations

The three-dimensional shallow water equations are given by:

$$\frac{\partial u}{\partial x} + \frac{\partial v}{\partial y} + \frac{\partial w}{\partial z} = 0 \tag{A.1a}$$

$$\frac{\partial u}{\partial t} + u\frac{\partial u}{\partial x} + v\frac{\partial u}{\partial y} + w\frac{\partial u}{\partial z} - fv = -\frac{1}{\rho}\frac{\partial p}{\partial x} + \frac{\partial}{\partial x}\left(A_h\frac{\partial u}{\partial x}\right) + \frac{\partial}{\partial y}\left(A_h\frac{\partial u}{\partial y}\right) + \frac{\partial}{\partial z}\left(A_v\frac{\partial u}{\partial z}\right) \tag{A.1b}$$

$$\frac{\partial v}{\partial t} + u\frac{\partial v}{\partial x} + v\frac{\partial v}{\partial y} + w\frac{\partial v}{\partial z} + fu = -\frac{1}{\rho}\frac{\partial p}{\partial y} + \frac{\partial}{\partial x}\left(A_h\frac{\partial v}{\partial x}\right) + \frac{\partial}{\partial y}\left(A_h\frac{\partial v}{\partial y}\right) + \frac{\partial}{\partial z}\left(A_v\frac{\partial v}{\partial z}\right) \tag{A.1c}$$

$$\frac{\partial p}{\partial z} = -\rho g \tag{A.1d}$$

Equation A.1d can be solved directly if assumed that ρ is independant of the depth z:

$$p = p_a + \rho g(H + \zeta - z) \tag{A.2}$$

Now equation A.1a can be integrated over the width of the domain to obtain width-averaged equations. Let

$$\hat{u}(x,z,t) = \frac{1}{B_2 - B_1}\int_{B_1}^{B_2} u\mathrm{d}y, \quad \hat{w}(x,z,t) = \frac{1}{B_2 - B_1}\int_{B_1}^{B_2} w\mathrm{d}y \tag{A.3}$$

$$\hat{\zeta}(x,t) = \frac{1}{B_2 - B_1}\int_{B_1}^{B_2} \zeta\mathrm{d}y \tag{A.4}$$

The Leibniz integration rule is defined as:

$$\frac{\partial}{\partial\alpha}\left(\int_a^b f\mathrm{d}\beta\right) = \int_a^b \frac{\partial f}{\partial\alpha}\mathrm{d}\beta + f|_b\frac{\partial b}{\partial\alpha} - f|_a\frac{\partial a}{\partial\alpha} \tag{A.5}$$

Now integrating over A.1a using equation A.5:

$$\int_{B_1}^{B_2}\frac{\partial u}{\partial x}+\frac{\partial v}{\partial y}+\frac{\partial w}{\partial z}\mathrm{d}y = 0 \tag{A.6a}$$

$$\Leftrightarrow\frac{\partial}{\partial x}\int_{B_1}^{B_2} u\mathrm{d}y - u|_{B_2}\frac{\partial B_2}{\partial x} + u|_{B_1}\frac{\partial B_1}{\partial x} + [v]_{B_1}^{B_2} + \frac{\partial}{\partial z}\int_{B_1}^{B_2} w\mathrm{d}y - w|_{B_1}\frac{\partial B_1}{\partial z} + w|_{B_2}\frac{\partial B_2}{\partial z} = 0 \tag{A.6b}$$

$$\Leftrightarrow\frac{\partial(B_2-B_1)\hat{u}}{\partial x}+\frac{\partial(B_2-B_1)\hat{w}}{\partial z} = \left[-u\frac{\partial B_1}{\partial x}+v\right]_{B_1}+\left[u\frac{\partial B_2}{\partial x}-v\right]_{B_2} \tag{A.6c}$$

$$\Leftrightarrow\frac{1}{B_2-B_1}\frac{\partial B_2-B_1}{\partial x}\hat{u}+\frac{\partial\hat{u}}{\partial x}+\frac{\partial\hat{w}}{\partial z}=0 \tag{A.6d}$$

Both B_1 and B_2 are independant of z thus the last two terms in (A.6b) disappear. Furthermore because of the boundary conditions (**??**) and (**??**) the right hand side of (A.6d) is equal to zero.
Now the second equation (A.1b) can be integrated over the width, the term fv is neglected in this equation because after averaging no water velocity in the y-direction should be present. Starting with the left-hand side:

$$\int_{B_1}^{B_2}\frac{\partial u}{\partial t}+\frac{\partial u^2}{\partial x}+\frac{\partial uv}{\partial y}+\frac{\partial uw}{\partial z}\mathrm{d}y \tag{A.7a}$$

$$= \frac{\partial}{\partial t}\int_{B_1}^{B_2} u\mathrm{d}y + \frac{\partial}{\partial x}\int_{B_1}^{B_2} u^2\mathrm{d}y + \frac{\partial}{\partial z}\int_{B_1}^{B_2} uw\mathrm{d}y + \left[u\left(u\frac{\partial B_1}{\partial x}-v\right)\right]_{B_1} + \left[-u\left(u\frac{\partial B_2}{\partial x}-v\right)\right]_{B_2} + uw|_{B_1}\frac{\partial B_1}{\partial z} - uw|_{B_2}\frac{\partial B_2}{\partial z} \tag{A.7b}$$

$$= (B_2-B_1)\frac{\partial\hat{u}}{\partial t}+\frac{\partial((B_2-B_1)\hat{u}^2)}{\partial x}+\frac{\partial((B_2-B_1)\hat{u}\hat{w})}{\partial z} \tag{A.7c}$$

In (A.7c) Again the boundary conditions (**??**) and (**??**) are used and the fact that B_1 and B_2 do not depend on z. Now the right-hand side can be integrated

as well:

$$\int_{B_1}^{B_2} -\frac{1}{\rho}\frac{\partial p}{\partial x} + \frac{\partial}{\partial x}\left(A_h\frac{\partial u}{\partial x}\right) + \frac{\partial}{\partial y}\left(A_h\frac{\partial u}{\partial y}\right) + \frac{\partial}{\partial z}\left(A_v\frac{\partial u}{\partial z}\right)\mathrm{d}y \tag{A.8a}$$

$$= \int_{B_1}^{B_2}\frac{1}{\rho}\left(\frac{\partial \rho}{\partial x}g(H+\zeta-z)+\rho g\frac{\partial \zeta}{\partial x}\right)\mathrm{d}y + \frac{\partial}{\partial x}\int_{B_1}^{B_2} A_h\frac{\partial u}{\partial x}\mathrm{d}y + \frac{\partial}{\partial z}\int_{B_1}^{B_2} A_v\frac{\partial u}{\partial z}\mathrm{d}y + \left[A_h\frac{\partial u}{\partial x}\frac{\partial B_1}{\partial x} + A_v\frac{\partial u}{\partial z}\frac{\partial B_1}{\partial z} - A_h\frac{\partial u}{\partial y}\right]_{B_1} + \left[-A_h\frac{\partial u}{\partial x}\frac{\partial B_2}{\partial x} - A_v\frac{\partial u}{\partial z}\frac{\partial B_2}{\partial z} + A_h\frac{\partial u}{\partial y}\right]_{B_2} \tag{A.8b}$$

$$= g(B_2-B_1)\frac{\partial \hat{\zeta}}{\partial x} + \int_{B_1}^{B_2}\frac{1}{\rho}\left(\frac{\partial \rho}{\partial x}g(H+\zeta-z)\right)\mathrm{d}y + \frac{\partial}{\partial x}\left((B_2-B_1)\hat{A}_h\frac{\partial \hat{u}}{\partial x}\right) + \frac{\partial}{\partial z}\left(\hat{A}_v\frac{\partial \hat{u}}{\partial z}\right)(B_2-B_1) + \left[A_h\frac{\partial u}{\partial x}\frac{\partial B_1}{\partial x} - A_h\frac{\partial u}{\partial y}\right]_{B_1} + \left[-A_h\frac{\partial u}{\partial x}\frac{\partial B_2}{\partial x} + A_h\frac{\partial u}{\partial y}\right]_{B_2} \tag{A.8c}$$

The third shallow water equation is not integrated in the width because it describes the velocity change in the y-direction, which is not present in the width-averaged shallow water equations.

Pertubation techniques for width-averaged shallow-water equations

Now all width-averaged shallow water equations have been calculated some assumptions are made to make the equations easier to work with. First of all, the functions describing the eddy viscocity coefficients in the horizontal direction A_h are assumed to be much smaller than one. Thus, in this case the terms containing this function can be removed from the equations.
Furthermore, the vertical eddy coefficent function A_v is assumed to be constant. The main reason for this is that the function can only be computed numerically which is almost impossible on such a large domain, a value can be assigned based on experimients.
Also for the sake of simplicity the density ρ is assumed to constant and equal to ρ_0. After removing all terms which can be neglected the width-averaged shallow water equations look like this:

$$\frac{\partial \hat{u}}{\partial x} + \frac{\partial \hat{w}}{\partial z} + \frac{1}{B_2-B_1}\frac{\partial (B_2-B_1)}{\partial x}\hat{u} = 0 \tag{A.9a}$$

$$\frac{\partial \hat{u}}{\partial t} + \frac{\partial \hat{u}^2}{\partial x} + \frac{\partial (\hat{u}\hat{w})}{\partial z} = g\frac{\partial \hat{\zeta}}{\partial x} + \hat{A}_v\frac{\partial^2 \hat{u}}{\partial z^2} \tag{A.9b}$$

Let $\delta(x) = \frac{1}{B_2-B_1}\frac{\partial (B_2-B_1)}{\partial x}$. The second width-averaged shallow water equation can be scaled to make it dimensionless, this is done so the seperated terms can

be compared better:

$$\begin{array}{rrrrr} \frac{\partial \hat{u}}{\partial t}+ & \frac{\partial \hat{u}^2}{\partial x}+ & \frac{\partial(\hat{u}\hat{w})}{\partial z}= & g\frac{\partial \hat{\zeta}}{\partial x}+ & \hat{A}_v\frac{\partial^2 \hat{u}}{\partial z^2} \\ 1+ & \frac{U}{\sigma L}+ & \frac{U}{\sigma L}= & \frac{gA_{M_2}}{\sigma UL}+ & \frac{\hat{A}_v}{\sigma H^2} \\ O(1)+ & O(\varepsilon)+ & O(\varepsilon)= & O(1)+ & O(1) \end{array}$$

Nondimentional term	Typical parameter	Order	Value
$\frac{\partial \hat{u}}{\partial t}$	1	1	1
$\frac{\partial \hat{u}^2}{\partial x}$	$\frac{U}{\sigma L}$	$O(\varepsilon)$	0.135
$\frac{\partial \hat{u}\hat{w}}{\partial x}$	$\frac{U}{\sigma L}$	$O(\varepsilon)$	0.135
$\frac{\partial \hat{\zeta}}{\partial x}$	$\frac{gA_{M_2}}{\sigma UL}$	$O(1)$	1.39
$\hat{A}_v\frac{\partial^2 \hat{u}}{\partial z^2}$	$\frac{A_v}{\sigma H^2}$	$O(1)$	0.857

Now writing $\hat{u} = \Re[(u_0(x,z)+\varepsilon u_1(x,z))e^{i\sigma t}]$, $\hat{w} = \Re[(w_0(x,z)+\varepsilon w_1(x,z))e^{i\sigma t}]$ and $\hat{\zeta} = \Re[(\zeta_0(x)+\varepsilon\zeta_1(x))e^{i\sigma t}]$ this set of equations can be solved for the leading order functions u_0, w_0 and ζ_0:

$$\frac{\partial u_0}{\partial x} + \frac{\partial w_0}{\partial z} + \delta(x)u_0 = 0 \tag{A.10a}$$

$$i\sigma u_0 - g\frac{\partial \zeta_0}{\partial x} + \hat{A}_v\frac{\partial^2 u_0}{\partial z^2} = 0 \tag{A.10b}$$

Solution to width-averaged leading-order shallow water equations

Now equation (A.10b) can be solved:

$$u_0(x,z) = C_1(x)\exp\left(\sqrt{\frac{A_v}{i\sigma}}z\right) + C_2(x)\exp\left(-\sqrt{\frac{A_v}{i\sigma}}z\right) \tag{A.11}$$

From boundary conditions (**??**) it follows that $C_1(x) = C_2(x)$, The other boundary condition gives:

$$u_0(x,z) = -\frac{g}{i\sigma}\frac{\partial \zeta_0}{\partial x}\left(1 - \frac{s\cosh(\beta z)}{A_v\beta\sinh(\beta H) + s\cosh(\beta H)}\right) \tag{A.12}$$

Where $\beta = \sqrt{\frac{A_v}{i\sigma}}$. Plugging this in equation (A.10a) gives:

$$\begin{aligned} w_0(x,z) = \frac{g}{i\sigma}\left(z - \frac{s\sinh(\beta z)}{A_v\beta^2\sinh(\beta H) + s\beta\cosh(\beta H)}\right)\left(\frac{\partial^2\zeta_0}{\partial x^2} + \delta(x)\frac{\partial\zeta_0}{\partial x}\right) \\ + \frac{g}{i\sigma}\frac{\partial\zeta_0}{\partial x}\frac{s\sinh\beta z(H_x A_v\beta\cosh\beta H + sH_x\sinh\beta H)}{2(A_v\beta\sinh\beta H + s\cosh\beta H)^2} + C3(x) \end{aligned} \tag{A.13a}$$

Using the first boundary condition of (**??**) gives $C_3(x) = \zeta_0 i\sigma$. Now assuming H is a constant and using the second boundary condition of (**??**) an ordinary differential equation for the water level ζ_0 can be constructed:

$$\frac{\partial^2 \zeta_0}{\partial x^2} + \delta(x)\frac{\partial \zeta_0}{\partial x} - \frac{\sigma^2}{g\gamma}\zeta_0 = 0 \tag{A.14}$$

Where:

$$\gamma = \frac{s \sinh \beta H}{A_v \beta^2 \sinh \beta H + s\beta \cosh \beta H} - H$$

In this case the general solution to ζ_0 is:

$$\zeta_0(x) = c_1 e^{\alpha_1 x} + c_2 e^{\alpha_2 x} \tag{A.15}$$

Where the integration constant α_1 and α_2 are equal to:

$$\alpha_1 = -\frac{\delta}{2} + \frac{\sqrt{\delta^2 + \frac{4\sigma^2}{g\gamma}}}{2} \quad , \alpha_2 = -\frac{\delta}{2} - \frac{\sqrt{\delta^2 + \frac{4\sigma^2}{g\gamma}}}{2} \tag{A.16}$$

In the case of a single inlet the functions c_1 and c_2 can be written as:

$$c_1 = \frac{-\alpha_2 A_{M_2} e^{\alpha_2 L}}{\alpha_1 e^{\alpha_1 L} - \alpha e^{\alpha_2 L}} \tag{A.17a}$$

$$c_2 = A_{M_2} + \frac{\alpha_2 A_{M_2} e^{\alpha_2 L}}{\alpha_1 e^{\alpha_1 L} - \alpha e^{\alpha_2 L}} \tag{A.17b}$$

Finally, with the double inlet system the functions c_1 and c_2 can be written as:

$$c_1(t) = A_{M_2} \tag{A.18a}$$

$$c_2(t) = \frac{A_{M_2}(e^{i\phi_{M_2}} - e^{\alpha_2 L})}{e^{\alpha_1 L} - e^{\alpha_2 L}} \tag{A.18b}$$

In a more general case, where H is not assumed to be constant, the ordinary differential equation cannot be solved exact. A finite difference scheme to solve ζ has to be used. The differential equation would look like:

$$T_1(x)\frac{\partial^2 \zeta_0}{\partial x^2} + T_2(x)\frac{\partial \zeta_0}{\partial x} + T_3(x)\zeta_0 = 0$$

Where:

$$T_1(x) = \frac{s \sinh \beta H(x)}{A_v \beta^2 \sinh \beta H(x) + s\beta \cosh \beta H(x)} - H(x) \tag{A.19a}$$

$$\begin{aligned} T_2(x) = \delta(x)T_1(x) + H_x(x)\left(1 - \frac{s \cosh \beta H(x)}{A_v \beta^2 \sinh \beta H(x) + s\beta \cosh \beta H(x)}\right) \\ + \frac{s \sinh \beta H(x)(H_x(x) A_v \beta \cosh \beta H(x) + s H_x(x) \sinh \beta H(x))}{2(A_v \beta^2 \sinh \beta H(x) + s\beta \cosh \beta H(x))^2} \end{aligned} \tag{A.19b}$$

$$T_3 = -\frac{\sigma^2}{g} \tag{A.19c}$$

A.1.2 Width-averaged concentration equation

Derivation of width-averaged concentration equation

The sediment concentration equation is given by:

$$\frac{\partial c}{\partial t}+\frac{\partial (uc)}{\partial x}+\frac{\partial (vc)}{\partial y}+\frac{\partial (c(w-w_s))}{\partial z}=\frac{\partial}{\partial x}\left(K_h\frac{\partial c}{\partial x}\right)+\frac{\partial}{\partial y}\left(K_h\frac{\partial c}{\partial y}\right)+\frac{\partial}{\partial z}\left(K_v\frac{\partial c}{\partial z}\right) \tag{A.20}$$

By integrating over the width of the channel the left hand side of this equation can be simplified to:

$$\begin{aligned}&\frac{\partial}{\partial t}\int_{B_1}^{B_2} c\mathrm{d}y+\frac{\partial}{\partial x}\int_{B_1}^{B_2} uc\mathrm{d}y+\frac{\partial}{\partial z}\int_{B_1}^{B_2} c(w-w_s)\mathrm{d}y\\ &\qquad+\left[c\left(v-\frac{\partial B_2}{\partial x}u\right)\right]^{B_2}+\left[-c\left(v-\frac{\partial B_1}{\partial x}u\right)\right]^{B_1} \qquad \text{(A.21a)}\\ =&(B_2-B_1)\frac{\partial \hat{c}}{\partial t}+\frac{\partial}{\partial x}((B_2-B_1)\hat{u}\hat{c})+(B_2-B_1)(\hat{c}(\hat{w}-w_s))\\ &\qquad+\left[c\left(v-\frac{\partial B_2}{\partial x}u\right)\right]^{B_2}+\left[-c\left(v-\frac{\partial B_1}{\partial x}u\right)\right]^{B_1} \qquad \text{(A.21b)}\end{aligned}$$

The right hand side of equation (A.20) can be integrated over the width in the same way:

$$\begin{aligned}&\frac{\partial}{\partial x}\int_{B_1}^{B_2} K_h\frac{\partial c}{\partial x}\mathrm{d}y+\frac{\partial}{\partial z}\int_{B_1}^{B_2} K_v\frac{\partial c}{\partial z}\mathrm{d}y+\left[K_h\left(\frac{\partial c}{\partial y}-\frac{\partial B_2}{\partial x}\frac{\partial c}{\partial x}\right)\right]^{B_2}\\ &\qquad+\left[-K_h\left(\frac{\partial c}{\partial y}-\frac{\partial B_1}{\partial x}\frac{\partial c}{\partial x}\right)\right]^{B_1} \qquad \text{(A.22a)}\\ &=\frac{\partial}{\partial x}\left((B_2-B_1)K_h\frac{\partial \hat{c}}{\partial x}\right)+(B_2-B_1)K_v\frac{\partial^2 \hat{c}}{\partial z^2}\\ &+\left[K_h\left(\frac{\partial c}{\partial y}-\frac{\partial B_2}{\partial x}\frac{\partial c}{\partial x}\right)\right]^{B_2}+\left[-K_h\left(\frac{\partial c}{\partial y}-\frac{\partial B_1}{\partial x}\frac{\partial c}{\partial x}\right)\right]^{B_1} \qquad \text{(A.22b)}\end{aligned}$$

All terms between brackets in equations (A.21b) and (A.22b) are equal to zero because there is no flux through the side boundary. Because of this $\overrightarrow{n}(c\overrightarrow{u}-K_h\overrightarrow{\nabla}c)=0$ where $\overrightarrow{n}=(-\frac{\partial B_1}{\partial x},1)$ at $y=B_1$ and $\overrightarrow{n}=(\frac{\partial B_2}{\partial x},-1)$ at $y=B_2$. Furthermore, let the fluctation terms c' and u' be written as $c'=c-\int_{B_1}^{B_2} c\mathrm{d}y$ and $u'=u-\int_{B_1}^{B_2} u\mathrm{d}y$. Then it is assumed that that correlations $\frac{\partial}{\partial x}\int_{B_1}^{B_2} u'c'\mathrm{d}y$ can be modeled as dispersive contribution thus become equal to zero. Thus, the width-averaged sediment concentration equation is equal to:

$$\frac{\partial \hat{c}}{\partial t}+\hat{u}\frac{\partial \hat{c}}{\partial x}+(\hat{w}-w_s)\frac{\partial \hat{c}}{\partial z}=\delta(x)K_h\frac{\partial \hat{c}}{\partial x}+K_h\frac{\partial^2 \hat{c}}{\partial x^2}+K_v\frac{\partial^2 \hat{c}}{\partial z^2} \tag{A.23}$$

Perturbation analysis of the width-averaged concentration equation

Now the width-averaged concentration equation is derived the main balance between the terms can be assessed. First of all, K_h and K_v are assumed to be equal to A_h and A_v. Thus, all terms with K_h are assumed to be equal to zero because $A_v << 1$. The equation now becomes:

$$\frac{\partial \hat{c}}{\partial t} + \hat{u}\frac{\partial \hat{c}}{\partial x} + (\hat{w} - w_s)\frac{\partial \hat{c}}{\partial z} = K_v \frac{\partial^2 \hat{c}}{\partial z^2} \tag{A.24}$$

Now making the equation dimensionless results in:

$$\frac{\partial \hat{c}}{\partial t} + \quad \hat{u}\frac{\partial \hat{c}}{\partial x} + \quad \hat{w}\frac{\partial \hat{c}}{\partial z} - \quad w_s\frac{\partial \hat{c}}{\partial z} = \quad K_v\frac{\partial^2 \hat{c}}{\partial z^2} \tag{A.25a}$$

$$1 + \quad \frac{U}{\sigma L} + \quad \frac{U}{\sigma L} - \quad \frac{w_s}{\sigma H} = \quad \frac{K_v}{\sigma H^2} \tag{A.25b}$$

$$O(1) + \quad O(\varepsilon) + \quad O(\varepsilon) - \quad O(1) = \quad O(1) \tag{A.25c}$$

Now write $\hat{c}(t,x,z) = c_0(t,x,z) + \varepsilon c_1(t,x,z)$. The leading order width-averaged sediment concentration equation is given by:

$$\frac{\partial c_0}{\partial t} - w_s\frac{\partial c_0}{\partial z} = K_v\frac{\partial^2 c_0}{\partial z^2} \tag{A.26}$$

Solution to leading order width-averaged concentration equation

By writing $c_0 = c^{00} + \Re(e^{2i\sigma t}c^{04})$ and using the Fourier series for $|u_0|$ equation (A.26) can be rewritten in two equations:

$$-w_s\frac{\partial c^{00}}{\partial z} = K_v\frac{\partial^2 c^{00}}{\partial z^2} \tag{A.27a}$$

$$2i\sigma c^{04} - w_s\frac{\partial c^{04}}{\partial z} = K_v\frac{\partial^2 c^{04}}{\partial z^2} \tag{A.27b}$$

$$\tag{A.27c}$$

The constituent c^{00} does not depend on t because the forcing term a_0 does not depend on t thus the derivative is zero. The boundary conditions for these equations are:

$$w_s c^{00} + K_v\frac{\partial c^{00}}{\partial z} - 0 \ \text{ at } z = 0, -K_v\frac{\partial c^{00}}{\partial z} = \frac{w_s\rho_s saa_0}{g'd_s} \ \text{ at } z = -H(x)$$

$$w_s c^{04} + K_v\frac{\partial c^{04}}{\partial z} - 0 \ \text{ at } z = 0, -K_v\frac{\partial c^{04}}{\partial z} = \frac{w_s\rho_s sa(a_2 - ib_2)}{g'd_s} \ \text{ at } z = -H(x)$$

This gives:

$$c^{00}(x,z) = \frac{\rho_s saa_0}{g'd_s}\exp\left(-\frac{w_s}{K_v}(H+z)\right) \tag{A.28a}$$

$$c^{04}(x,z) = A\left(-\frac{w_s - \lambda}{w_s + \lambda}\exp\left(-\frac{w_s + \lambda}{2K_v}\right) + \exp\left(-\frac{w_s - \lambda}{2K_v}\right)\right) \tag{A.28b}$$

Where $\lambda = \sqrt{w_s + 8i\sigma K_v}$ and

$$A = \frac{w_s \rho_s \frac{sa(a_2 - ib_2)}{g' d_s}}{-\frac{w_s - \lambda}{2} \exp\left(\frac{w_s + \lambda}{2K_v} H\right) + \frac{w_s - \lambda}{2} \exp\left(\frac{w_s - \lambda}{2K_v} H\right)}$$

A.1.3 Morphodynamic Equilibrium Condition

The time evolution equation for the bed reads:

$$-\rho_s (1 - p) \frac{\partial H}{\partial t} = D - E_s \tag{A.29}$$

where p is defined by the porosity of the sediment and D and E_s are given by the deposition of sediment and erosion of the seabed. The result from equation (A.22b) and (A.21b) can be used to find a relation between D and E_s. First, (A.22b) and (A.21b) are depth averaged:

$$\begin{aligned}\frac{\partial}{\partial t} \int_{-H}^{\zeta} (B_2 - B_1) \hat{c} \mathrm{d}z + \frac{\partial}{\partial x} \int_{-H}^{\zeta} (B_2 - B_1) \hat{u} \hat{c} \mathrm{d}z - \frac{\partial}{\partial x} \int_{-H}^{\zeta} K_h (B_2 - B_1) \frac{\partial \hat{c}}{\partial x} \mathrm{d}z = \\ -(B_2 - B_1) \left[w_s \hat{c} + K_h \frac{\partial \hat{c}}{\partial x} \frac{\partial H}{\partial x} + K_v \frac{\partial \hat{c}}{\partial z} \right]^{-H} + (B_2 - B_1) \left[\frac{\partial \hat{\zeta}}{\partial t} + \hat{u} - \hat{w} \right]^{\zeta} \\ +(B_2 - B_1) \hat{c} \left[\hat{u} \frac{\partial H}{\partial x} + \hat{w} \right]^{-H} + (B_2 - B_1) \left[w_s \hat{c} - K_h \frac{\partial \hat{c}}{\partial x} \frac{\partial \hat{\zeta}}{\partial x} + K_v \frac{\partial \hat{c}}{\partial z} \right]^{\zeta}\end{aligned} \tag{A.30a}$$

Because of boundary conditions (**??**) and (**??**) and the fact that there is no flux through the sea surface the last three terms of the right hand side of (A.30a) are equal to zero.
Deposition flux normal to the seabed is defined by the term:

$$D = w_s \hat{c} n_z \tag{A.31}$$

The erosional sediment flux is given by:

$$E_s = -K_h \overrightarrow{\nabla} c - K_v \frac{\partial c}{\partial z} \overrightarrow{n_z} \tag{A.32}$$

By integrating over the width this equation becomes $E_s = -K_h \frac{\partial \hat{c}}{\partial x} n_x - K_v \frac{\partial \hat{c}}{\partial z} n_z$. The normal vector components are given by $n_x = \frac{1}{|\overrightarrow{n}|} \frac{\partial H}{\partial x}$ and $n_z = \frac{1}{\overrightarrow{n}}$. This gives the relation:

$$\begin{aligned}(B_2 - B_1)(-D + E_s) = \frac{\partial}{\partial t} \int_{-H}^{\zeta} (B_2 - B_1) \hat{c} \mathrm{d}z \\ +\frac{\partial}{\partial x} \int_{-H}^{\zeta} (B_2 - B_1) \hat{u} \hat{c} \mathrm{d}z - \frac{\partial}{\partial x} \int_{-H}^{\zeta} K_h (B_2 - B_1) \frac{\partial \hat{c}}{\partial x} \mathrm{d}z\end{aligned} \tag{A.33a}$$

Bibliography

[1] Waterdata — rijkswaterstaat. https://www.rijkswaterstaat.nl/water/waterdata-en-waterberichtgeving/waterdata. Accessed: 2021-04-02.

[2] R. L. Brouwer, H. M. Schuttelaars, and P. C. Roos. Modelling the influence of spatially varying hydrodynamics on the cross-sectional stability of double inlet systems. *Ocean Dynamics*, 63(11-12):1263–1278, 2013. Cited By :8.

[3] H. de Swart. Physics of coastal systems. 2009.

[4] X. Deng, C. Meerman, T. Boelens, T. D. Mulder, P. Salles, , and H. M. Schuttelaars. Morphodynamic equilibria in double inlet systems: their existence and stability. 2021.

[5] C. Meerman, V. Rottschäfer, and H. Schuttelaars. Influence of geometrical variations on morphodynamic equilibria in short tidal basins. *Ocean Dynamics*, 69(2):221–238, 2019. Cited By :1.

[6] B. R. Munson, D. F. Young, and T. H. Okiishi. Fundamentals of fluid mechanics. 1994. Cited By :1395.

[7] A. B. Murray. Contrasting the goals, strategies and predictions associated with simplified numerical models and detailed simulation. 2003.

[8] J. Pedlosky. Geophysical fluid dynamics. 1979. Cited By :2126.

[9] H. Schuttelaars. *Evolution and Stability Analysis of Bottom Patterns in Tidal Embayments*. 1997.

[10] H. M. Schuttelaars and H. E. De Swart. Idealized long-term morphodynamic model of a tidal embayment. *European Journal of Mechanics, B/Fluids*, 15(1):55–80, 1996. Cited By :72.

[11] M. ter Brake. *Tidal Embayments*. 2011.

[12] J. van de Kreeke. Can multiple tidal inlets be stable? *Estuarine, Coastal and Shelf Science*, 30(3):261–273, 1990. Cited By :45.

[13] L. van Rijn. Principles of sediment transport in rivers, estuaries and coastal seas. 1993.